

AN ABSTRACT OF THE THESIS OF

Grahme T Williams for the degree of Master of Science in Civil Engineering presented on September 2, 2005.

Title: Investigation of the Fatigue Behavior of Diagonally-Cracked CRC Deck-Girders Repaired with CFRP.

Abstract approved:

Redacted for privacy

Christopher C. Higgins

Fiber reinforced polymers (FRP) are becoming more widely used for repair and strengthening of conventionally reinforced concrete (CRC) bridge members. Once installed, the repair may be exposed to millions of load cycles during service life. The anticipated life of FRP repairs for shear strengthening of bridge members under repeated service loads is uncertain. Field and laboratory tests of FRP repaired CRC deck-girders were performed to evaluate high-cycle fatigue behavior. An in-service 1950's vintage CRC deck-girder bridge repaired with externally bonded carbon fiber laminates for shear strengthening was inspected and instrumented. FRP strain data were collected under ambient traffic conditions. In addition, eight full-size girder specimens repaired with bonded carbon fiber laminate for shear strengthening were tested in the laboratory under repeated loads. Results indicated relatively small in-situ FRP strains,

laboratory fatigue loading produced localized debonding along the FRP termination locations at the stem-deck interface, the fatigue loading did not significantly alter the ultimate capacity of the specimens.

© Copyright by Grahme T. Williams
September 2, 2005
All Rights Reserved

Investigation of the Fatigue Behavior of Diagonally-Cracked CRC Deck-Girders
Repaired with CFRP

by
Grahme T. Williams

A THESIS

submitted to

Oregon State University

in partial fulfillment of
the requirements for the
degree of

Master of Science

Presented September 2, 2005
Commencement June 2006

Master of Science thesis of Grahme T. Williams presented on September 2, 2005.

APPROVED:

Redacted for privacy

Major Professor, representing Civil Engineering

Redacted for privacy

Head of the Department of Civil, Construction and Environmental Engineering

Redacted for privacy

Dean of the Graduate School

I understand that my thesis will become part of the permanent collection of Oregon State University libraries. My signature below authorizes release of my thesis to any reader upon request.

Redacted for privacy

Grahme T. Williams, Author

ACKNOWLEDGMENTS

This research was funded by the Oregon Department of Transportation and Federal Highway Administration and overseen by research coordinator Mr. Steven Soltesz. All repair materials and procedures were donated by MBrace of Cleveland, Ohio and Pioneer Waterproofing of Portland, Oregon with the help of Mr. Neil Antonini. The help of both of these individuals is greatly appreciated. Reinforcing steel and fabrication were donated by Cascade Steel Rolling Mills of McMinnville, Oregon and Farwest Steel of Eugene, Oregon, respectively. The authors would also like to thank Dr. Tanarat Potisuk, Mr. Richard Forrest, Mr. Thomas Schumacher, Ms. Michelle Chavez, and Ms. Angela Rogge for their assistance in experimental testing and data reduction. The findings and conclusions are those of the authors and do not necessarily reflect those of the project sponsors or the individuals acknowledged.

CONTRIBUTION OF AUTHORS

Dr. Christopher Higgins assisted with testing, data collection, and data interpretation.

He also assisted with the design and writing of Chapters 2 and 3.

TABLE OF CONTENTS

	<u>Page</u>
CHAPTER 1: General Introduction	1
CHAPTER 2: Full-Scale Tests of Diagonally Cracked CRC Deck–Girders Repaired with CFRP	2
Biographical Sketch of Authors	3
Keywords.....	3
Abstract.....	3
Introduction	4
Research Significance	5
Experimental Program.....	6
Test Specimens.....	6
Specimen Variables.....	10
Testing Method.....	12
Experimental Results.....	17
Conclusions	25
Acknowledgements	28
Notation	29
References	30

TABLE OF CONTENTS (Continued)

	<u>Page</u>
CHAPTER 3: Fatigue of Diagonally-Cracked CRC Girders Repaired with	
CFRP	33
Abstract.....	34
CE Database Subject Headings	35
Introduction	35
Background.....	36
Field Study.....	38
Ambient Traffic Induced CFRP Strains	42
Laboratory tests	44
Test Specimens.....	44
Test Variables.....	47
Testing Method.....	50
Experimental Results.....	54
Conclusions	62
Acknowledgements	64
Notation.....	65
References	66
CHAPTER 4: General Conclusion.....	73
BIBLIOGRAPHY	75

LIST OF FIGURES

<u>Figure</u>	<u>Page</u>
2.1 Specimen configurations	7
2.2 Test setup.....	11
2.3 Instrumentation.....	11
2.4 Cracked specimens and internal steel strain gages.....	13
2.5 Repaired specimen configuration and corresponding failure crack	15
2.6 Midspan deformation response	16
2.7 Bond regions of primary load carrying CFRP u-wraps across failure cracks .	19
2.8 (a) Strain Measurements, (b) Diagonal deformation of failure crack region ..	21
3.1 Willamette River Bridge overall plan and elevation and main girder details	39
3.2 CFRP repairs to a) main girders and b) bent caps.	40
3.3 Field measured cracking, embedded stirrups, and externally bonded CFRP on exterior girder	41
3.4 Schematic of instrumentation locations.....	42
3.5 Strain range-number of cycles measured under ambient traffic conditions at all instrumented locations.....	43
3.6 Equivalent constant amplitude strain ranges for all instrumented locations ..	43
3.7 Typical specimen details	45
3.8 Precrack and failure test setup.....	48
3.9 Fatigue test setup	49
3.10 Typical instrumentation layout.....	49

LIST OF FIGURES (Continued)

<u>Figure</u>	<u>Page</u>
3.11 CFRP repair layout, fatigue damage, and failure cracks and debonding	52
3.12 Midspan displacement response comparison of specimens prior to and after fatigue loading.....	56
3.13 Change in crack size range for various fatigue loading ranges	56
3.14 Diagonal deformation response of IT specimens	57
3.15 Internal steel reinforcing strain reduction due to application of CFRP shear repair	58
3.16 Representative strains measured during fatigue loading	59

LIST OF TABLES

<u>Table</u>	<u>Page</u>
2.1 Experimental summary.....	7
2.2 Internal steel reinforcing properties.....	8
2.3 Concrete and CFRP bond properties and maximum initial diagonal crack size.....	9
2.4 Composite material properties: Reported and experimental	10
3.1 Steel reinforcing property description	46
3.2 Concrete and CFRP bond properties and maximum initial diagonal crack size.....	46
3.3 Composite material properties: Reported and experimental	47
3.4 Experimental summary.....	54

General Introduction

Many 1950's CRC deck girder bridges remain in the national inventory and are reaching the end of their originally intended design lives. Field inspections in Oregon revealed that large numbers of these bridges exhibited significant diagonal cracks in the girders and bent caps (ODOT 2002). Over-estimation of the concrete contribution to shear resistance during design, reduced anchorage requirements for flexural steel, increasing service load magnitudes and volume, as well as shrinkage and temperature effects, may contribute to diagonal cracking of the bridge members.

With the large population of cracked bridges and limited resources available for replacements, effective repair methods are needed. Many strengthening techniques for CRC elements have been introduced and studied, including the use of externally bonded steel plates, post-tensioning, and internal and external supplemental stirrups, among others. Externally bonded carbon fiber reinforced plastics (CFRP) are becoming more widely used and accepted for repair and strengthening of concrete members. CFRPs offer the potential for increased strength and stiffness, they have a relatively simple installation process, are resistant to corrosion from deicing chlorides, and contribute little additional weight to the member. However, the anticipated life of these CFRP repairs under repeated service loads is uncertain and research was undertaken to investigate the life of diagonally-cracked RCDG bridges repaired with CFRP.

Full-Scale Tests of Diagonally Cracked CRC Deck-Girders Repaired with CFRP

Grahme T. Williams and Christopher C. Higgins

American Concrete Institute Structural Journal
P.O. Box 9094
Farmington Hills, MI 48333-9094
To be published

Full-Scale Tests of Diagonally Cracked CRC Deck–Girders Repaired with CFRP

Grahme T. Williams¹ and Christopher C. Higgins²

Biographical Sketch of Authors

¹ Design Engineer, Parsons Brinckerhoff, Melbourne, Australia (Former Graduate Research Assistant, Dept. of Civil, Construction and Environmental Engineering, Oregon State University, Corvallis, OR 97331)

²Associate Professor, Dept. of Civil, Construction and Environmental Engineering, Oregon State University, Corvallis, OR 97331

Keywords

Bridges, carbon fiber, CFRP, full-scale testing, reinforced concrete, repair, shear

Abstract

The use of fiber reinforced plastics (FRP) is growing as a repair and strengthening technique for conventionally reinforced concrete (CRC) bridge elements. Much of the existing data regarding performance of members repaired with FRP has been gathered through testing of reduced-scale specimens. This investigation reports experimental results for five full-scale shear deficient reinforced concrete deck girders (RCDG) built to reflect 1950's vintage proportions, materials, and details. Specimens were loaded to

produce diagonal cracks, repaired for shear with carbon fiber reinforced plastic (CFRP) u-wraps, and tested to failure. Results indicate the repaired members provide additional shear capacity and improve ductility even with large debonded regions prior to failure. The repairs also increased the member stiffness.

Introduction

Many 1950's CRC deck girder bridges remain in the national inventory and are reaching the end of their originally intended design lives. Field inspections in Oregon revealed that large numbers of these bridges exhibited significant diagonal cracks in the girders and bent caps (ODOT 2002). Over-estimation of the concrete contribution to shear resistance during design, reduced anchorage requirements for flexural steel, increasing service load magnitudes and volume, as well as shrinkage and temperature effects, may contribute to diagonal cracking of the bridge members. With the large population of cracked bridges and limited resources available for replacements, effective repair methods are needed. Many strengthening techniques for CRC elements have been introduced and studied, including the use of externally bonded steel plates, post-tensioning, and internal and external supplemental stirrups, among others. Externally bonded carbon fiber reinforced plastics (CFRP) are becoming more widely used and accepted for repair and strengthening of concrete members. CFRPs offer the potential for increased strength and stiffness, they have a relatively simple installation process, are resistant to corrosion from deicing chlorides, and contribute little additional weight to the member.

A significant amount of previous research exists on the behavior of CRC elements strengthened for shear with CFRP laminates (Chajes *et al.* 1995, Malvar *et al.* 1995, Sato 1996, Norris *et al.* 1997, Triantafillou 1998, Czaderski 2000, Kachlakev and McCurry 2000, Shehata *et al.* 2000, Al-Mahaidi *et al.* 2001, Li *et al.* 2001, Chen and Teng 2003). A very limited amount of this work has been done using full-scale specimens. Reduced-scale models may not adequately reflect realistic strain fields in large size members and limit the available development length for both reinforcing steel and FRP. The current design guide for FRP systems applied to structural concrete in the United States (ACI 440.2R-02 (2002)) recognizes the current lack of data on large size elements in the introduction: “the design basis is the result of research primarily conducted on moderately sized and proportioned members” (ACI 440 2002). Other important factors for FRP applications to in-service members include incorporation of existing service level cracking as well as treatment of realistic reinforcement details such as flexural rebar cutoffs and variable stirrup spacing.

Research Significance

Large numbers of shear deficient CRC deck-girder bridges remain in service. A significant number exhibit diagonal cracking and there is concern regarding their ability to sustain the increasing volume and weight of modern truck traffic. Limited resources preclude wholesale replacements, and retrofit with CFRP offers the potential for extending their service life. Limited data is currently available and design approaches

have not been fully validated regarding the performance of shear deficient full-size CRC girders repaired with CFRP. This paper provides details of an experimental program for five diagonally-cracked full-size CRC girders using realistic 1950's stirrup and flexural details repaired with CFRP for shear.

Experimental Program

Test Specimens

Five specimens were tested monotonically to study the behavior of 1950's vintage CRC deck bridge girders repaired for shear using CFRP u-wraps. Specimens were designed at full scale with considerations made for typical details and material properties. The behavior and capacity of the unrepaired specimens were well characterized based on previous work done by Higgins *et al.* (2004). Two designs were used to test both positive (T-beam) and negative moment bending regions (inverted-T (IT)) with various flexural bar cut-off, hook, and stirrup spacing details as seen in Fig. 2.1. Specimens were initially loaded to produce diagonal cracking representative of that observed from field inspections of existing Oregon highway bridges. They were then repaired with CFRP, and finally, tested to failure. The unrepaired shear strengths were predicted using the computer program *Response 2000* (Bentz 2000), which predicted the actual unrepaired member capacity to within 2% with a coefficient of variation of under 8% for a series of 44 similar full-size CRC specimens (Higgins *et al.* 2004). The estimated unrepaired shear capacities for the specimens are shown in Table 2.1.

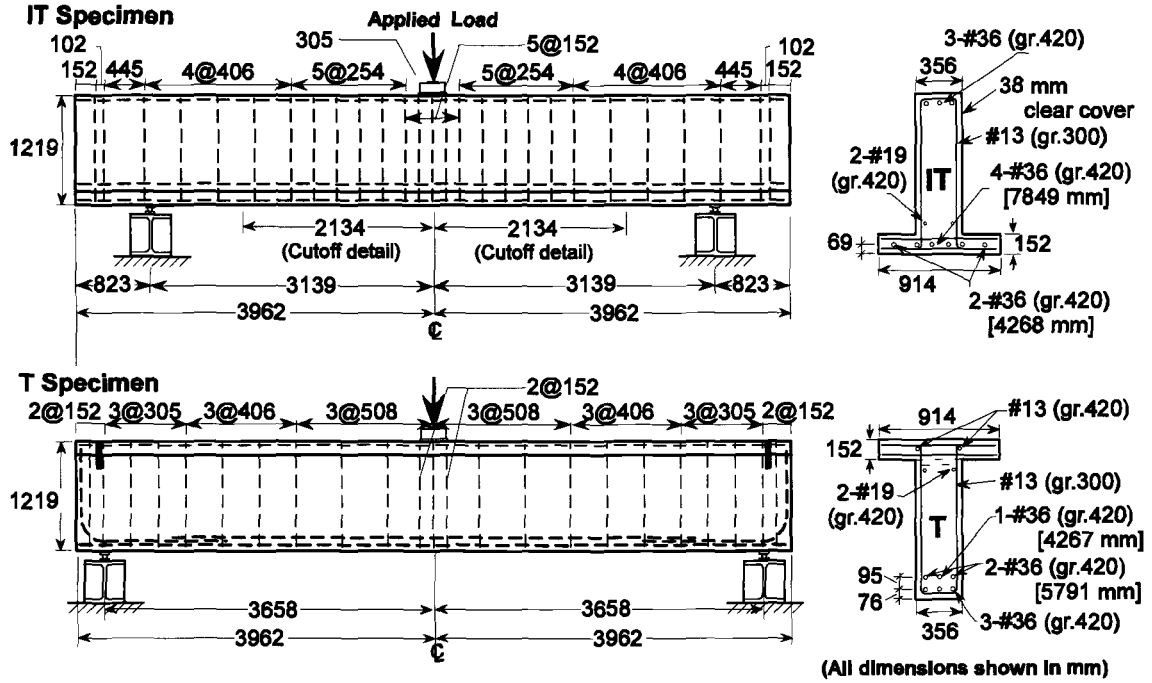


Fig. 2.1: Specimen configurations

Table 2.1: Experimental summary

Specimen	Failure Mode	V_{Pred} (kN)	V_{APP} (kN)	θ_{ck} (deg)	$\mu\epsilon_{max}$	f_{bond} (Mpa)
1IT01	Shear / Compression	919	1145	37	4930	0.70
1IT02	Shear / Compression	918	1112	37	8708	1.23
2T04	Shear / Compression	599	1225	40	4424	1.46
4IT07	Shear / Tension	888	1110	44	4073	1.57
4IT08	Shear / Compression	877	865	23	3812	-

All specimens were cast with the same cross-sectional geometry. Members had a height of 1219 mm (48 in.) with a stem width of 356 mm (14 in.) and a deck portion 914 mm (36 in.) wide by 152 mm (6 in.) thick as depicted in Fig. 2.1. Reinforcing bars for all of the specimens were from the same heats and tension tests were conducted to determine material properties, as summarized in Table 2.2. ASTM A615 Grade 420 (60 ksi) steel was used for the longitudinal reinforcing, with Grade 300 (40 ksi) steel for the stirrups. The stirrup grade is representative of intermediate grade steel used in the 1950's. A concrete mix design was used which produced compressive strengths similar to core samples obtained from ODOT bridges of around 24 MPa (3500 psi). The 28-day and day-of-test compressive strengths are shown in Table 2.3.

Table 2.2: Internal steel reinforcing properties

Description	Bar Size	Grade	f_y (MPa)	f_{ult} (MPa)
Stirrups	# 13	300	350	559
Deck	# 13	420	443	724
Skin	# 19	420	461	648
Flexure	# 36	420	481	717
Hooks	# 36	420	481	717

Table 2.3: Concrete and CFRP bond properties and maximum initial diagonal crack size

Specimen	f'_c (MPa)		Initial Max Crack Size (mm)	CFRP Bond Strength (MPa)
	28-Day	Failure		
1IT01	28.06	29.30	0.635	3.50
1IT02	26.27	26.34	1.016	2.02
2T04	26.27	29.37	0.762	1.82
4IT07	23.51	26.27	1.016	0.74
4IT08	22.89	23.10	1.270	1.23

All repairs were done using unidirectional high strength carbon fiber fabric applied in a wet lay-up procedure. Two different fibers were used with individual component and composite properties shown in Table 2.4. Composite properties were determined from unidirectional tension tests performed for each fiber thickness as per ASTM 3039 (2001) recommendations. Pull-off tests of the CFRP were performed to determine bond strength for each specimen. Test results are shown in Table 2.3 and exhibited wide scatter.

Table 2.4: Composite material properties: Reported and experimental

Property	Individual Component*			Composite [†]			
	Saturant	Carbon Fiber		CF130		CF160	
		CF130	CF160	Mean	St Dev	Mean	St Dev
Thickness, t (mm/ply)	-	0.165	0.33	0.975	0.134	1.47	0.16
Ultimate Tensile Strength (MPa)	55.2	3800	3800	717	94	846	151
Ultimate Tensile Strength per Unit Width (kN/mm/ply)	-	0.625	1.25	0.692	0.042	1.22	0.13
Tensile Modulus (MPa)	3034	227000	227000	38750	4530	54400	7020
Ultimate Rupture Strain, %	3.5	1.67	1.67	1.85	0.11	1.55	0.18

*Master Builders, Inc. 2001 material vendor specifications.

[†]Average and standard deviation values obtained from 20 composite samples of each fiber type tested in accordance with ASTM D 3039/D 3039M.

Specimen Variables

All tests were conducted using a three-point loading configuration as shown in Fig. 2.2. Inverted-T (IT) specimens were tested at a span length of 6280 mm (20.6 ft) between centerline of supports for both initial and failure loading schemes and the T-beam was tested at 7315 mm (24 ft) span. Force was applied through a 3560 kN (800 kip) capacity hydraulic cylinder operating on a 69 MPa (10,000 psi) system. The applied force was measured with a 2670 kN (600 kip) capacity load cell and was distributed through a 25 mm (1 in.) thick, 305 mm (12 in.) square steel plate. End reactions were provided through 102 mm (4 in.) wide steel plates resting on 51 mm (2 in.) diameter steel rollers, supported on steel beams attached to the strong-floor. High-strength grout was applied to the interface between the steel plates and concrete beams to ensure uniform bearing areas.

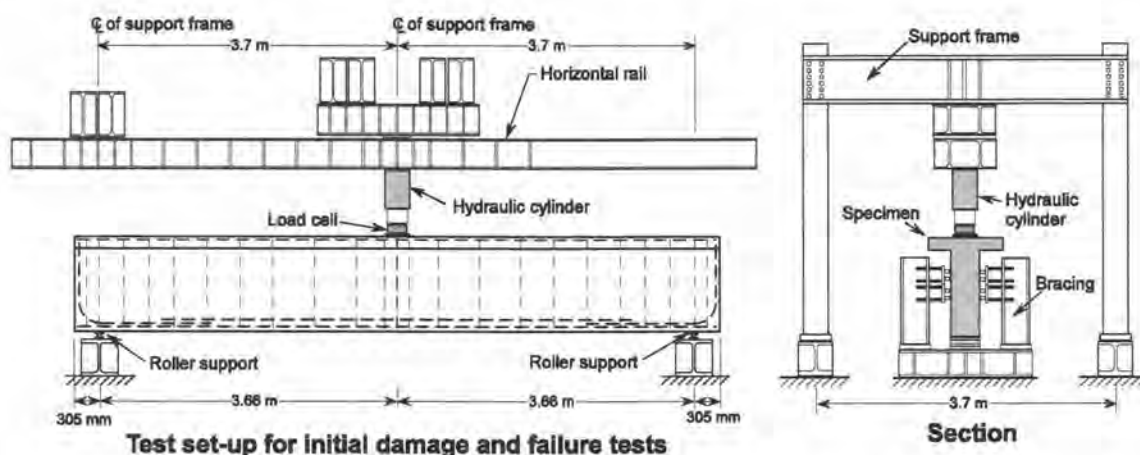


Fig. 2.2: Test setup

Instrumentation was installed to capture local and global behaviors. Strain gages were used to monitor internal steel reinforcing and external CFRP strains, displacement transducers were used to measure diagonal deformations, local crack motions, and support displacements at each corner of the reaction plates, and string potentiometers were used to measure centerline displacement. Typical instrumentation is illustrated in Fig. 2.3.

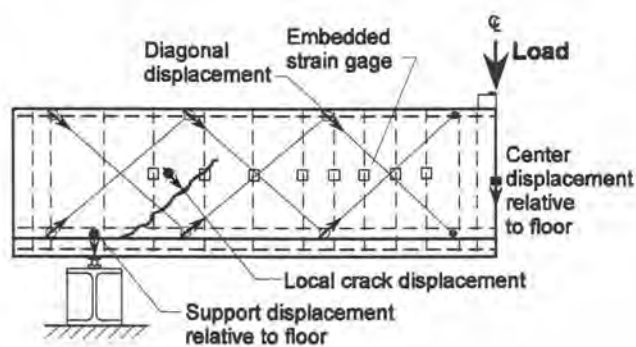


Fig. 2.3: Instrumentation

Testing Method

An initial loading protocol was performed to induce diagonal cracking representative of in-service CRC girders, based on field measured values from previous research (Higgins *et al.* 2004). Maximum diagonal crack sizes after loading of each beam are shown in Table 2.3, and ranged from 0.635 – 1.27 mm (0.025 – 0.05 in.). After reaching the desired level of cracking, the applied load was removed from all but one specimen. The subsequent crack patterns are shown in Fig. 2.4. Specimen 1IT01 was held at an applied load of 356 kN (80 kips) after reaching the desired level of diagonal cracking to study the influence of superstructure dead load during repair. The dead load magnitude is representative of the service-level dead load shear near an interior support location for a typical 1950's vintage three-span continuous CRC deck-girder bridge having 15.2 m (50 ft) spans and a uniform dead load of 23.3 kN/m/girder (1.6 kip/ft/girder). The applied laboratory dead load moment was somewhat higher than the service-level bridge dead load moment due to the span geometry.

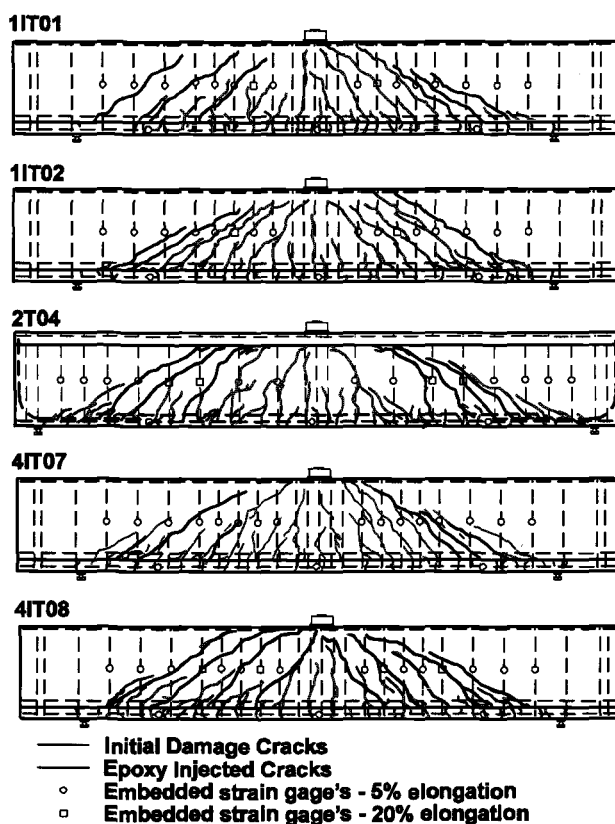


Fig. 2.4: Cracked specimens and internal steel strain gages

Once girders were diagonally cracked, a commercially available CFRP unidirectional high strength carbon fiber fabric laminate system was applied to the specimens. The entire repair procedure was performed by a qualified contractor with experienced personnel. Cracks were inspected and all significant diagonal cracks were injected with a high-strength epoxy resin and allowed to cure. It should be noted that not all visible cracks were injected, just those of sufficient width necessary to allow material to flow between the crack surfaces. The beams were then surfaced with a diamond bit grinder to remove loose concrete and expose surface voids. A primer was applied to the concrete surface. Once the primer was dry, putty and then saturant were applied to the surface.

While both of these were wet, the carbon fiber was cut and applied to the specified locations, being worked into place with a soft trowel until the fibers were saturated. A final layer of saturant was then applied.

Upon reaching the manufacturer recommended curing time, the specimens were instrumented and tested to failure. U-wrap laminate locations on each specimen are shown in Fig. 2.5. A 406 mm (16 in.) gap was used between CFRP strips at midspan of each IT specimen to simulate the transverse bent cap location in a bridge structure, where CFRP could not be applied. Specimens 1IT01 and 1IT02 were repaired with a single layer of 305 mm (12 in.) wide CF130 laminate spaced 256 mm (14 in.) on-center. This allows a 51 mm (2 in.) gap between strips to permit visual identification of cracking in the concrete stem and is representative of what is done in the field. Specimen 1IT01 was loaded in 188 kN (40 kip) increments, followed by unloading to a minimum of 222 kN (50 kips) until failure. All other specimens were loaded in 222 kN (50 kip) increments followed by unloading to a minimum of 22 kN (5 kips) until failure. The overall load-deflection responses for all specimens are shown in Fig. 2.6.

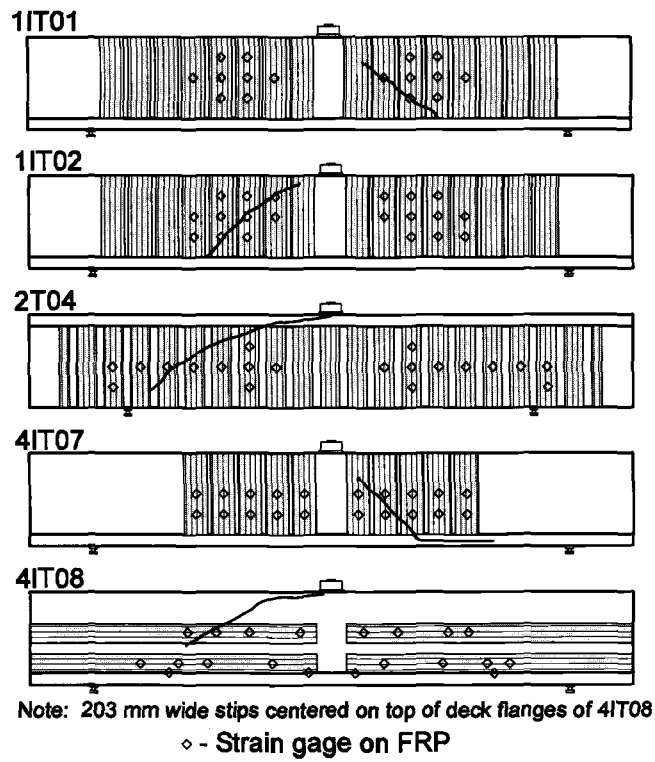


Fig. 2.5: Repaired specimen configuration and corresponding failure crack

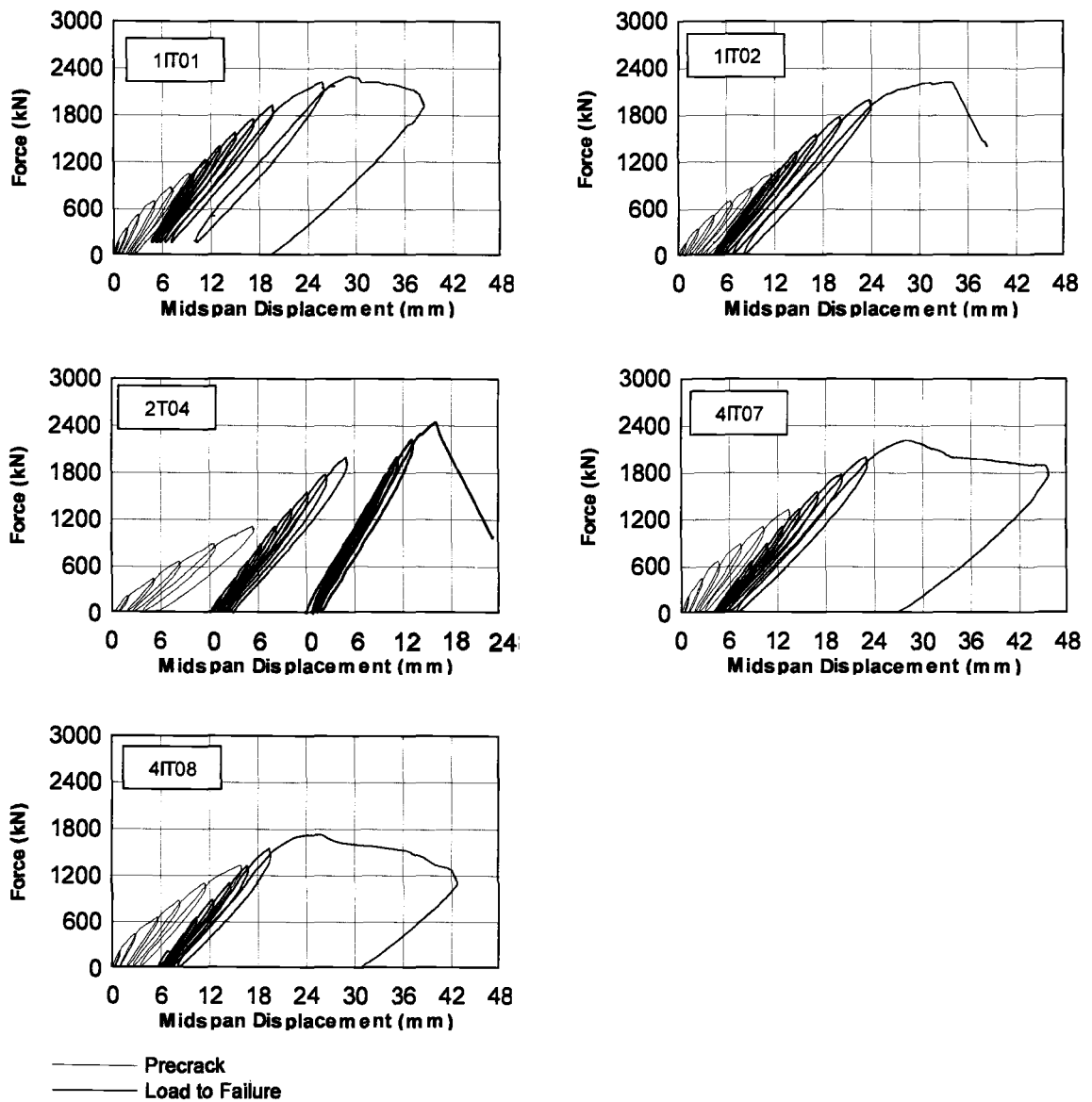


Fig. 2.6: Midspan deformation response

Specimen 2T04 was repaired with a single layer of 254 mm (10 in.) wide CF160 laminate. For specimen 2T04, support locations were initially placed at 7315 mm (24 ft) and loaded to 2000 kN (450 kips). Member response did not exhibit signs of shear failure even as the flexible capacity was approached. The supports were moved to 6280

mm (20.6 ft) and the specimen was loaded to 2000 kN (450 kips), again without evidence of shear failure. Thus, the support spacing was again shortened to 5334 mm (17.5 ft) and the specimen was loaded to failure.

A targeted repair approach was used on specimen 4IT07 to attempt to produce a different failure mode or location than observed for specimens 1IT01 and 1IT02. The CFRP material was applied to a finite area (high shear and high moment region) rather than over the entire span. Laminate strips were a single layer of 305 mm (12 in.) wide CF160 spaced 256 mm (14 in.) on-center. The same unidirectional CF160 laminate was used to retrofit specimen 4IT08, but was applied with the fibers oriented horizontally rather than vertically. Four 254 mm (10 in.) wide strips were applied to each face of the web as shown in Fig. 5 and two 203 mm (8 in.) wide strips were applied in the center of the top surface of the deck flange on each side of the web. A gap between the longitudinal strips was again used to simulate the bent cap location whereby the strips cannot be continuous.

Experimental Results

The performance of each of the repaired specimens was evaluated through load-deflection response, internal stirrup and external CFRP strains, flexural reinforcement demands, and crack width growth. Global and local demands were compared before and after the specimens were repaired to assess the effect of CFRP on the internal stress distribution. Upon reloading after repair, cracking was observed along the previously

epoxy injected diagonal cracks and occurred at approximately the same load levels as the original diagonal cracks. Debonding of the CFRP u-wraps was monitored in areas of terminations and at diagonal crack locations. As the applied load increased on all specimens, loud popping and snapping was heard as the strips progressively debonded from the web along the strip termination in the flexural tension zone and along the edges of the diagonal cracks. In all specimens partial debonding was observed to occur progressively. Even portions of the span that did not contain the failure crack had debonded strips and peeling from the surface of the concrete web. The progressive debonding of the multiple strips over the loading history provided a quasi-ductile response. Debonded areas were easily detectable by infrared thermography, by visual inspection, and sounding the CFRP strips. Compared with adequately bonded strip areas, the debonded areas tended to have a lower, hollow sound when the surface was tapped, similar to that from the commonly used "chain-drag" technique used to identify delaminations in concrete decks. All specimens exhibited significant CFRP debonding, and a single remaining CFRP strip crossed the diagonal crack prior to failure (upon debonding of that strip). The debonding and peeling away of the CFRP strips at failure was a noticeable indicator of imminent failure. This progressive debonding provided a quasi-ductile response in that some amount of deformation was achieved as the maximum load remained constant. Further, the progressive debonding of the CFRP strips provides some of the philosophical intent behind the designer's desire for ductile response: warning of impending collapse.

The diagonal failure crack for the CFRP repaired specimens was generally observed to be at a steeper angle than those observed previously in similar unrepaired CRC girders (Higgins *et al.* 2004). None of the specimens exhibited fiber rupture. As fiber rupture did not occur at failure, the bond strength controlled the strength of the CFRP u-wraps. The condition of the single u-wrap remaining across the diagonal failure crack for each specimen prior to failure is shown in Fig. 2.7. The average bond stress (determined from the bonded area shown in Fig. 2.7) necessary to develop the measured CFRP strains at mid height of the u-wrap are shown in Table 2.1. Comparison of the average bond stress developed at the diagonal crack with the pull-off bond strength tests shown in Table 2.3 indicate that the actual bond stress developed in the specimens was below that measured in the pull-off tests except for specimen 4IT07 (discussed subsequently).

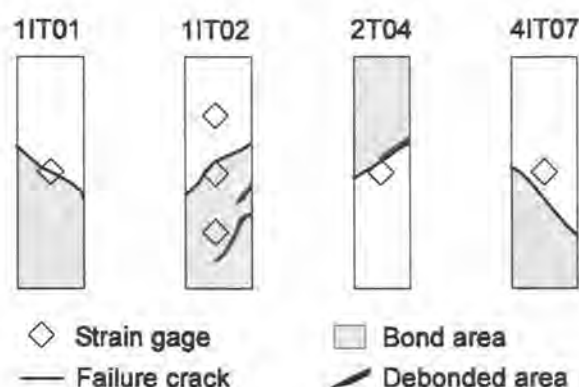


Fig. 2.7: Bond regions of primary load carrying CFRP u-wraps across failure cracks

Specimens 1IT01 and 1IT02 were used to study the effect of dead load during repair procedures. Both specimens were repaired with identical material size, ply, layout, and procedure. The applied shear force at failure for specimen 1IT01 and 1IT02 were 1145 kN (258 kips) and 1112 kN (250 kips), respectively. The difference of 33 kN (8 kips) in

applied shear force at failure showed little overall difference between the specimens. For the sufficiently ductile stirrup reinforcement and flexural details, the level of dead load did not significantly impact overall member capacity. Strain gage readings for the internal stirrups and the external CFRP u-wraps at nearly the same location, mid-height along the diagonal failure cracks, for Specimen 1IT01 exhibited strain compatibility over much of the loading history, as shown in Fig. 2.8(a). The strains in the stirrup and the CFRP were similar until a load of approximately 2060 kN (463 kips). Afterward the CFRP strain increased at a higher rate than the proximate stirrups. In contrast, specimen 1IT02 showed a lack of strain compatibility between the internal stirrup and the CFRP. As seen in Fig. 2.8(a), the strain in the CFRP was higher than that of the stirrup at each particular load step. A difference in performance between these two specimens was also seen from the diagonal deformations across the failure crack as shown in Fig. 2.8(b). Specimen 1IT01 exhibited less deformation, and was stiffer, than specimen 1IT02. This was also seen in the midspan displacement of the two specimens in Fig. 2.6.

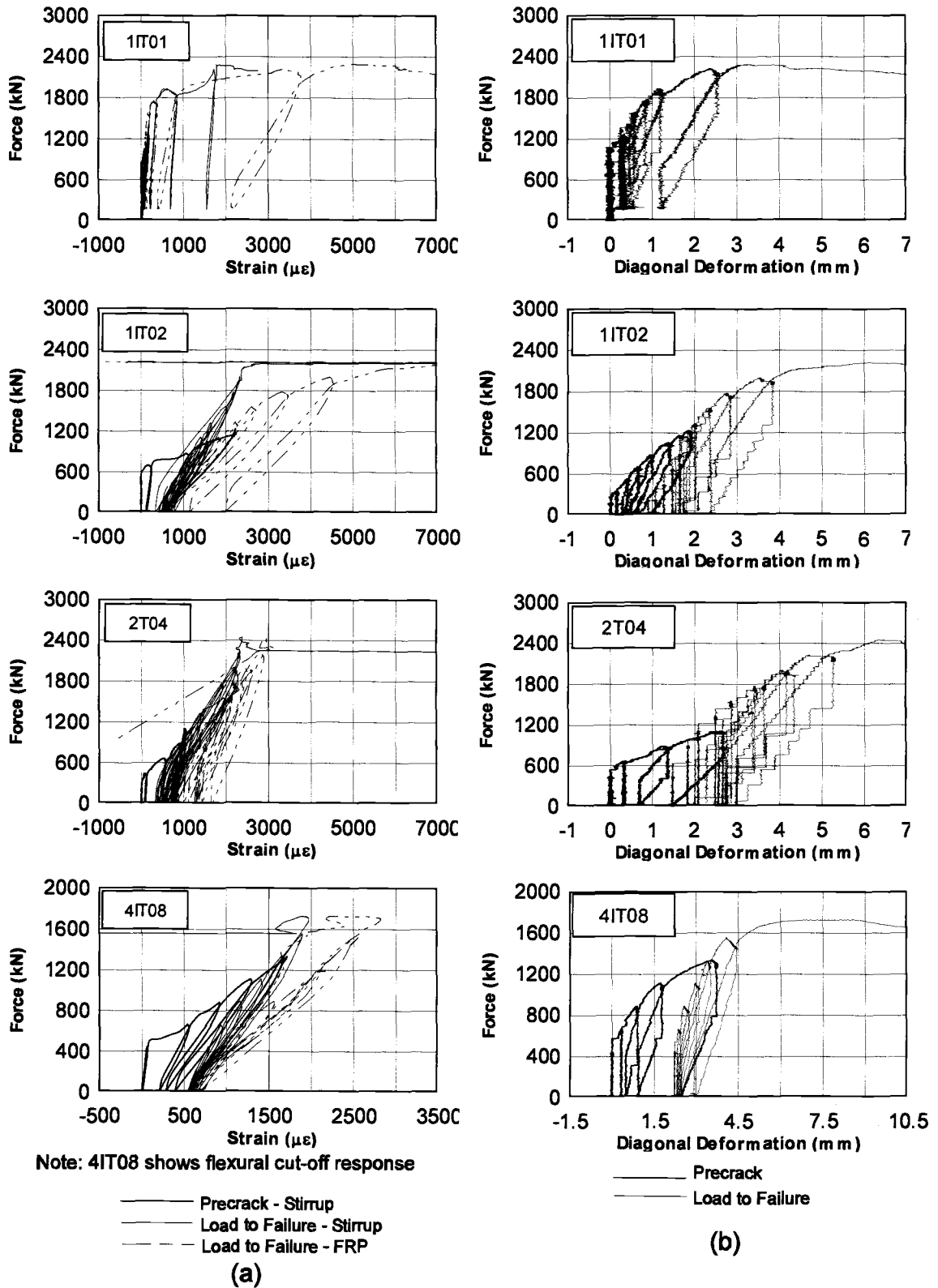


Fig. 2.8: (a) Strain Measurements, (b) Diagonal deformation of failure crack region

Specimen 2T04 was the only test performed with the CFRP material applied to the positive bending region. During the load test to failure using the original span configuration, minimal CFRP debonding was observed and the flexural capacity was approached. To investigate the behavior of the CFRP in a shear dominated failure mode, the span length was shortened to preclude flexural failure. In Fig. 2.6, three different midspan displacement response curves show the behavior of the specimen during the precrack and at the two different span lengths subsequent to repair. A much stiffer response was observed by the addition of the CFRP laminate repair and by the shortened span length as shown in the midspan displacement behavior and also in the individual CFRP strains. In the different support configurations, the CFRP strains were smaller at corresponding load steps when the specimen had smaller moment for the same shear magnitude. This indicates CFRP repaired members exhibit shear-moment interaction that may lend itself to sectional analysis methods such as modified compression field theory.

Example measured stirrup and CFRP strains across the failure diagonal crack show an uneven distribution in Fig. 2.8(a). The strains were larger in the CFRP than the stirrup at each load step. Also of interest, the diagonal deformation of the specimen across the failure crack in Fig. 2.8(b) showed larger values than any of the other specimens, but the deformations decreased upon unloading. Large regions of the CFRP material were observed to be debonded from the concrete surface, although the specimen continued to

carry additional load. Upon reaching the peak load, the applied force was held as the CFRP u-wraps were observed to debond initiating from the strip termination located at the deck/stem interface and peeling away from the stem. After several strips had debonded, a single remaining CFRP strip crossing (one side of the web only) the diagonal crack debonded, resulting in sudden failure. The diagonal crack angle was approximately at 40° from horizontal and initially would have crossed three of the CFRP u-wraps.

Specimen 4IT07 used a targeted repair scheme based on the observed response of specimen 1IT02. The goal of the repair was to achieve similar capacity or a different failure mode using CFRP material applied to only a portion of the specimen. The applied shear at failure was 1110 kN (250 kips) and similar to specimen 1IT02 although failure initiated by anchorage loss at the flexural bar cut-off location. The diagonal failure crack was 44° from horizontal. Splitting cracks were observed at the deck edge and large sections of concrete spalled off the bottom of the deck near the cutoff location. Strain behavior of the stirrups and CFRP, as well as the diagonal deformation across the failure crack, were similar to those observed for specimen 1IT02. The flexural anchorage failure indicates that designers must recognize and address the increased demands placed on the often poor flexural details when shear capacity of existing structures is increased using FRP.

The strain behavior of the thicker CFRP material on specimen 4IT07 compared with specimen 1IT01 was significant even though the CFRP strip strength was not fully realized due to flexural anchorage failure. Prior to failure, specimen 4IT07 showed much less debonding and less cracking and popping of the CFRP was heard as the applied load increased compared with specimen 1IT02 (having the thinner CFRP). At failure, a smaller portion of the remaining load carrying strip was bonded in specimen 4IT07 than in 1IT02 (Fig. 2.7), yet it was carrying similar force. It is evident that the thicker material (CF160) requires a higher bond stress than does the thinner (CF130) CFRP to develop the force in the strip of similar width (even if the CFRP strains are smaller) as seen in Table 2.1. The thicker CFRP material also exhibited the lowest pull-off strengths (Table 2.3), indicating the thicker material may permit higher bond strengths (in shear) due to the higher stiffness which reduces strains at the bond interface. Additional work is required to further validate this observation for shear dominated response.

Specimen 4IT08 was repaired using only longitudinal CFRP strips in the flexural tension zone. Strain readings of the continuous flexural bars at the flexural cut-off detail are shown along with the strain in the CFRP applied to the deck soffit directly above the end of the cut-off bar in Fig. 2.8(a). As seen in this figure, the CFRP exhibited higher strains than the adjacent flexural reinforcing bars. At an applied load of 1334 kN (300 kips), the strains in the flexural bars were only slightly less than that observed during the precrack phase (unrepaired). Considering the diagonal deformation response shown

in Fig. 2.8(b), the addition of the CFRP strips did reduce the amount of diagonal cracking compared to the unrepaired specimen at precracking, although there was no increase in shear capacity. The final failure crack on specimen 4IT08 was observed to develop slowly. As the applied shear increased, the crack continued to open further causing debonding and bending of the fibers in the CFRP strips at the diagonal crack locations. Addition of longitudinal CFRP alone was not effective in increasing shear capacity due to debonding and fiber bending at diagonal crack locations. Addition of transverse CFRP strips may improve the response for the longitudinal strips and this combination enable the longitudinal strips to better reduce flexural demands that cutoff locations. Additional study is required to validate this concept.

Conclusions

Laboratory tests were performed on five CRC deck girders built to reflect 1950's vintage proportions, materials, and details at near static conditions. Specimens were precracked, repaired with CFRP strips, and tested to failure while monitoring global and local member responses. Factors considered included flexural cut-off details, variable stirrup spacing, dead load, positive and negative moment bending, and different repair configurations. Based on the experimental observations, the following conclusions are presented:

- Superimposed dead load of the magnitude considered (typical for moderate span vintage RCDG bridges) and with ductile stirrups did not impact the ultimate strength of the specimens. For longer span bridges with higher dead to live load ratios or different material properties, the impact of dead load could be significant.
- Repair schemes for shear using discrete CFRP strips provided a significant increase in ultimate strength capacity compared to unrepaired members.
- Specimen response after repair was noticeably stiffer in terms of midspan displacement and diagonal deformations.
- The repaired members exhibited strain compatibility between external CFRP strips and internal stirrups. Addition of the CFRP strips reduced the live-load demand in the internal stirrups at similar load levels.
- Repair for shear using CFRP must recognize the impact of the increased shear capacity on the flexural demands to prevent anchorage failures at flexural bar cut-off and anchorage details.
- Failure was controlled by debonding of CFRP strips initiating near the deck/stem interface.
- Thicker CFRP material exhibited reduced amounts of debonding and cracking and achieved higher bond stress than the thinner material.
- It was possible to increase the member shear strength using a targeted repair approach applying CFRP material only to a critical section rather than over the entire member.

- The CFRP repaired members tended to exhibit steeper crack angles than similar unrepaired specimens. At the point of failure, only one u-wrap was still acting across the failure crack.
- Prior to failure, significant areas of debonded CFRP material were observed. Progressive debonding of the multiple strips over the loading history provided a visual indication of distress prior to failure.
- Addition of longitudinal CFRP strips did not increase capacity due to debonding and bending of fibers at the poorly constrained diagonal cracks. The combined effect of longitudinal and transverse strips was not investigated, although some synergistic benefits are anticipated.

Acknowledgments

This research was funded by the Oregon Department of Transportation and Federal Highway Administration and overseen by research coordinator Mr. Steven Soltesz. All repair materials and procedures were donated by MBrace of Cleveland, Ohio and Pioneer Waterproofing of Portland, Oregon with the help of Mr. Neil Antonini. The help of both of these individuals is greatly appreciated. Reinforcing steel and fabrication were donated by Cascade Steel Rolling Mills of McMinnville, Oregon and Farwest Steel of Eugene, Oregon, respectively. The authors would also like to thank Dr. Tanarat Potisuk, Mr. Richard Forrest, Mr. Thomas Schumacher, Ms. Michelle Chavez, and Ms. Angela Rogge for their assistance in experimental testing and data reduction. The findings and conclusions are those of the authors and do not necessarily reflect those of the project sponsors or the individuals acknowledged.

Notation

The following symbols are used in this paper:

- f_{bond} = bond strength demand of CFRP on concrete surface (MPa);
- f'_c = compressive strength of concrete (MPa);
- f_{ult} = ultimate stress of internal reinforcing steel (MPa);
- f_y = yield stress of internal reinforcing steel (MPa);
- St Dev = standard deviation of measured CFRP properties;
- V_{APP} = applied shear from actuator (kN);
- V_{Pred} = predicted shear capacity using *Response 2000*TM (kN);
- $\mu\varepsilon_{\text{max}}$ = maximum measured CFRP strain at mid height of u-wrap ($\mu\varepsilon$); and
- θ_{ck} = angle of diagonal failure crack (degrees).

References

1. ODOT, "Oregon's Bridges 2002." Oregon Department of Transportation, http://www.odot.state.or.us/tsbbridgepub/PDFs/Senate_05_16_02.pdf (May 16, 2002), Salem, Oregon.
2. Chajes, M. J., Januszka, T.F., Mertz, D.R., Thomson, T.A., Finch, W.W., "Shear Strengthening of Reinforced Concrete Beams Using Externally Applied Composite Fabrics," *ACI Structural Journal*, v. 92, No. 3, May-June 1995, pp. 295-303.
3. Malvar, L.J., Warren, G.E., Inaba, C., "Rehabilitation of Navy Pier Beams with Composite Sheets," *Proceedings of the Second International RILEM Symposium*, August 23-25, 1995, pp. 533-540.
4. Sato, Y., Ueda, T., Kakuta, Y., Tanaka, T., "Shear Reinforcing Effect of Carbon Fiber Sheet Attached to Side of Reinforced Concrete Beams," *Advanced Composite Materials in Bridges and Structures*, 1996, pp. 621-627.
5. Norris, T., Saadatmanesh, H., Ehsani, M.R., "Shear and Flexural Strengthening of R/C Beams with Carbon Fiber Sheets," *ASCE Journal of Structural Engineering*, v. 123, No. 7, July 1997, pp. 903-911.
6. Triantafillou, T.C., "Shear Strengthening of Reinforced Concrete Beams Using Epoxy-Bonded FRP Composites," *ACI Structural Journal*, v. 95, No.2, March-April 1998, pp. 107-115.

7. Czaderski, C., EMPA, Swiss Federal Laboratories for Materials Testing and Research, "Shear Strengthening of Reinforced Concrete with CFRP," 45th International SAMPE Symposium, May 21-25, 2000, pp. 880-894.
8. Kachlakev, D., McCurry, D.D., "Behavior of Full-Scale Reinforced Concrete Beams Retrofitted for Shear and Flexural with FRP Laminates," *Composites Part B: Engineering*, v. 31, no. 6-7, 2000, pp. 445-452.
9. Shehata, E., Morphy, R., Rizkalla, S., "Fibre Reinforced Polymer Shear Reinforcement for Concrete Members: Behaviour and Design Guidelines," *Canadian Journal of Civil Engineering*, v. 27, no. 5, October 2004.
10. Al-Mahaidi, R., Lee, K., Taplin, G., "Behavior and Analysis of RC T-Beams Partially Damaged in Shear and Repaired with CFRP Laminates," *Structures Congress*, ASCE, Washington DC, May 2001.
11. Li, A., Assih, J., Delmas, Y., "*Shear* Strengthening of RC Beams with Externally Bonded CFRP Sheets," *ASCE Journal of Structural Engineering*, v. 127, No. 4, April 2001, pp. 374-380.
12. Chen, J.F., Teng, J.G., "Shear Capacity of Fiber-Reinforced Polymer-Strengthened Reinforced Concrete Beams: Fiber Reinforced Polymer Rupture," *ASCE Journal of Structural Engineering*, v. 129, No. 5, May 2003, pp. 615-625.
13. ACI 440.2R-02, American Concrete Institute, "Guide for the Design and Construction of Externally Bonded FRP Systems for Strengthening Concrete Structures." Farmington Hills, Michigan, 2002.

14. Higgins, C., Miller, T.H., Rosowsky, D.V., Yim, S.C., Potisuk, T., Daniels, T.K., Nicholas, B.S., Robelo, M.J., Lee, A-Y, and R.W. Forrest, "Research Project SPR 350 SR 500-91: Assessment Methodology for Diagonally Cracked Reinforced Concrete Deck Girders," Oregon Department of Transportation, Salem, OR, October 2004.
15. Bentz, E., (2000), Response 2000, University of Toronto,
<<http://www.ecf.utoronto.ca/~bentz/r2k.htm>>.
16. Master Builders, Inc., "MBrace Composite Strengthening System Material Specifications," Cleveland, OH, 2001.
17. ASTM D 3039/D 3039M-00, American Society of Testing and Materials, "Standard Test Method for Tensile Properties of Polymer Matrix Composite Materials," ASTM, West Conshohocken, PA, 2001.

Fatigue of Diagonally-Cracked CRC Girders Repaired with CFRP

Grahme T. Williams and Christopher C. Higgins

American Society of Civil Engineers Bridge Journal
1801 Alexander Bell Dr.
Reston, VA 20191
To be published

Fatigue of Diagonally-Cracked CRC Girders Repaired with CFRP

By Grahme Williams¹ and Christopher Higgins, P.E., M. ASCE²

Abstract

Fiber reinforced plastics (FRP) are becoming more widely used for repair and strengthening of conventionally reinforced concrete (CRC) bridge members. Once repaired, the member may be exposed to millions of load cycles during its service life. The anticipated life of FRP repairs for shear strengthening of bridge members under repeated service loads is uncertain. Field and laboratory tests of FRP repaired CRC deck-girders were performed to evaluate high-cycle fatigue behavior. An in-service 1950's vintage CRC deck-girder bridge repaired with externally bonded carbon fiber laminates for shear strengthening was inspected and instrumented. FRP strain data were collected under ambient traffic conditions. In addition, three full-size girder specimens repaired with bonded carbon fiber laminate for shear strengthening were tested in the laboratory under repeated loads and compared with two unfatigued specimens. Results indicated relatively small in-situ FRP strains, laboratory fatigue loading produced localized debonding along the FRP termination locations at the stem-deck interface, and the fatigue loading did not significantly alter the ultimate capacity of the specimens.

CE Database Subject Headings

Reinforced concrete, bridges, shear, field testing, fatigue, fiber reinforced polymer

Introduction

The national bridge inventory contains large numbers of CRC bridges that are lightly reinforced for shear. One of the most common types of CRC bridges is the deck-girder bridge (RCDG) used widely during the highway expansion of the late 1940's through the early 1960's. Many RCDG bridges are reaching the end of their originally intended design lives and the combined effects of over-estimation of allowable concrete shear stress at design, reduced anchorage requirements for flexural steel, increasing service load magnitudes and volume, as well as shrinkage and temperature effects, may contribute to diagonal tension cracking in these bridges. Due to the relatively light shear reinforcement, diagonal cracks may not be well constrained and therefore become quite wide. Repeated loading may further cause cracks to widen. Inspections of approximately 1,800 vintage RCDG bridges in Oregon by Oregon Department of Transportation (ODOT) personnel revealed over 500 with varying levels of diagonal cracking. As a result, a repair program was initiated to extend the service lives of these bridges. One type of repair material being used is externally bonded carbon fiber reinforced polymer (CFRP) laminates. The anticipated life of these CFRP repairs under repeated service loads is uncertain and research was undertaken to investigate the life of diagonally-cracked RCDG bridges repaired with CFRP.

Background

High-cycle fatigue behavior of CRC beams in shear is influenced by the concrete, reinforcing steel, and the interaction between the concrete and reinforcing steel. Previous research on high-cycle fatigue of concrete structures has focused on plain concrete, fatigue of beams, and reinforcing steel (ACI SP-41, 1974; ACI SP-75, 1982; ACI Committee 215, 1992). Fatigue tests of concrete beams without shear reinforcement were conducted by Chang and Kesler (1958). Shear fatigue of concrete beams with stirrups was investigated by Hawkins (1974), Ueda and Okamura (1981, 1983), as well as Kwak and Park (2001). Fatigue tests of deep beams were performed by Teng *et al.* (1998). Bond fatigue (between rebar and concrete) was studied by Rehm and Eligehausen (1979) and Balazs (1998). High-cycle fatigue of reinforcing steel was studied by Hanson *et al.* (1968), Hanson *et al.* (1974), Helgason and Hanson (1974), Jhamb and MacGregor (1974), Corley *et al.* (1978), and Kreger *et al.* (1989). Fatigue cracks tend to initiate at the transverse rib along the surface of the bar and the fatigue behavior depends on the stress conditions, reinforcing bar geometry including deformation height, base radius, width and bar diameter, as well as material properties (Hanson *et al.*, 1974; ACI-215, 1992). Fatigue life has generally been expressed in terms of the stress range (Hanson *et al.*, 1974). The current ACI specification (ACI-318, 2002) does not address fatigue of reinforcing steel, although ACI Committee 215 (1992) recommends a maximum service-level stress range, σ_r (MPa), for straight deformed reinforcing bars of:

$$\sigma_r = 161 - 0.33\sigma_{\min} \quad (3.1)$$

where σ_{\min} (MPa) is the minimum stress with tension taken as positive and compression taken as negative. The σ_r need not be taken as less than 138 MPa (20 ksi). The current AASHTO provisions (2002) specify a maximum stress range at service loads with impact be calculated as:

$$\sigma_r = 145 - 0.33\sigma_{\min} + 55 \frac{r}{h} \quad (3.2)$$

where σ_{\min} (MPa) is the minimum stress as defined previously, and r/h is the ratio of the base radius to transverse deformation height. When the r/h ratio is not known, a value of 0.3 is recommended.

Previous laboratory investigation involving fatigue response of externally bonded FRP laminates has focused primarily on flexural conditions (Muszynski and Sierakowski 1996, Papakonstantinou *et al.* 2001, Lopez *et al.* 2003, Breña *et al.* 2005). Some research has also been done on in-situ bridges repaired with FRP (Tedesco *et al.* 1996) through monitoring conditions both before and after repair showing stiffer member response and decreased stress of the reinforcing steel.

The fatigue behavior of full-sized RC bridge girders repaired with FRP for shear under realistic service-level stress ranges has not previously been investigated. Strain ranges in the CFRP of repaired in-service CRC deck-girder bridges are not known and the susceptibility of these repairs to damage under high-cycle fatigue is uncertain (ACI 440 2002).

Field Study

A deck-girder bridge designed in 1954 was investigated in the field testing portion of this research program. The Willamette River bridge (*Bridge Inventory Number 08156*) is located on Oregon Highway 219, near Newberg, OR. Inspection of the bridge in late summer of 2001 indicated significant diagonal cracking in the high-shear regions near the supports. The bridge consists of ten spans: four steel plate girder spans over water and three conventionally reinforced concrete approach spans at each end. Concrete approach spans exhibited significant diagonal cracks and were repaired using externally bonded fiber-reinforced polymer materials after completion of the initial inspection. The bridge has a regular layout with rectangular prismatic girders and the south approach spans were selected for instrumentation. The approach spans have three equal span lengths, 16.8 m (55 ft) each, and have a total width of 10.7 m (35 ft) as illustrated in Fig. 3.1. The spans are comprised of one simple span having five girders 368x1346 mm (14.5x53 in) and two continuous spans having four girders 330x1346 mm (13x53 in). Reinforced concrete diaphragms 229x1219 mm (9x48 in) are located at quarter points of each span. The approach spans have three simple supports and are continuous over one interior support with a transverse bent cap 419x1803 mm (16.5x71 in) supported by two columns. The specified concrete compression strength was 22.75 MPa (3300 psi) and reinforcing steel consisted of ASTM A305 intermediate grade deformed square and round bars with nominal yield stress of 276 MPa (40 ksi). The bridge was repaired primarily for shear with CFRP in the fall of 2001. The material used was CF130 unidirectional high-strength carbon fiber fabric, manufactured by MBrace. Prior

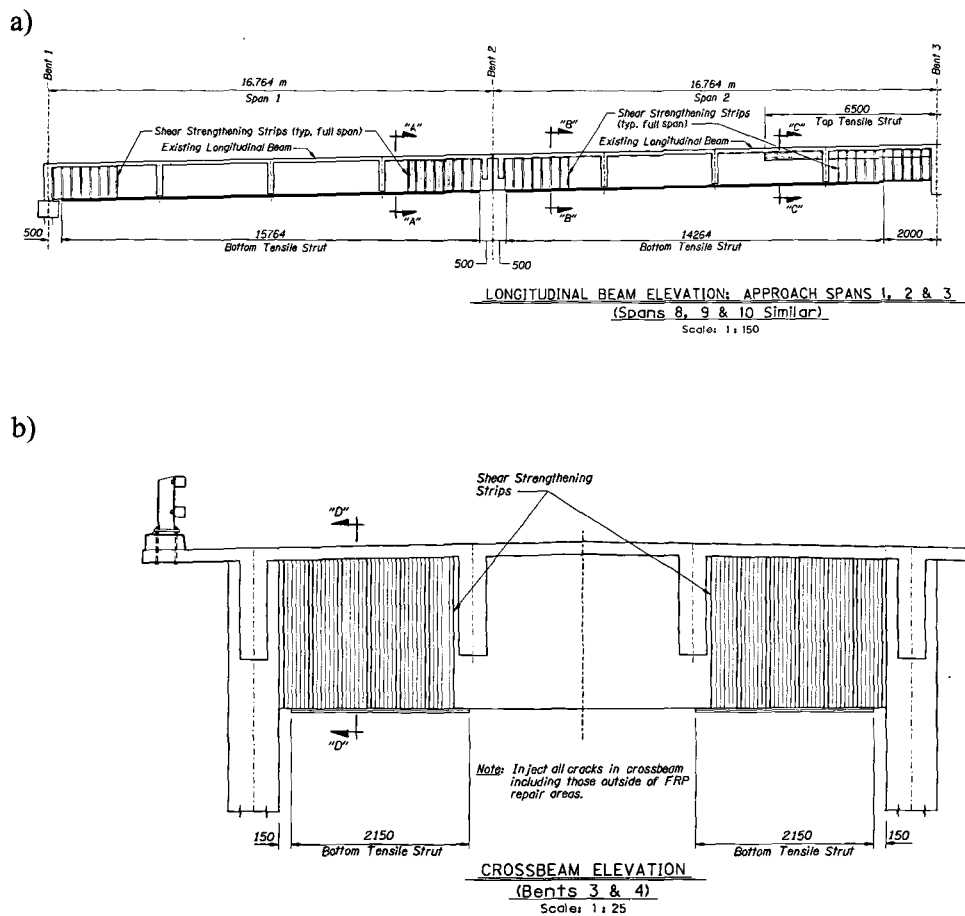


Fig. 3.2: CFRP repairs to a) main girders and b) bent caps

In October 2004, three years after installation of the CFRP repairs, the bridge was re-inspected, instrumented, and monitored under ambient traffic conditions to measure in-situ CFRP strain ranges at high shear locations. The bent caps and longitudinal deck girders were re-inspected to determine if cracking re-occurred and to identify the as-built locations of the CFRP strips. A Leica Disto Pro⁴ hand-held laser distance meter was used to rapidly locate cracks and CFRP strips relative to support locations. Examples of stirrup locations, original cracks, and CFRP strips, on the exterior girder,

are shown in Fig. 3.3. During the post-repair inspection, no new diagonal cracks were observed in the bent caps or girders. Flexural cracking was observed at only one location near midspan of the exterior girder.

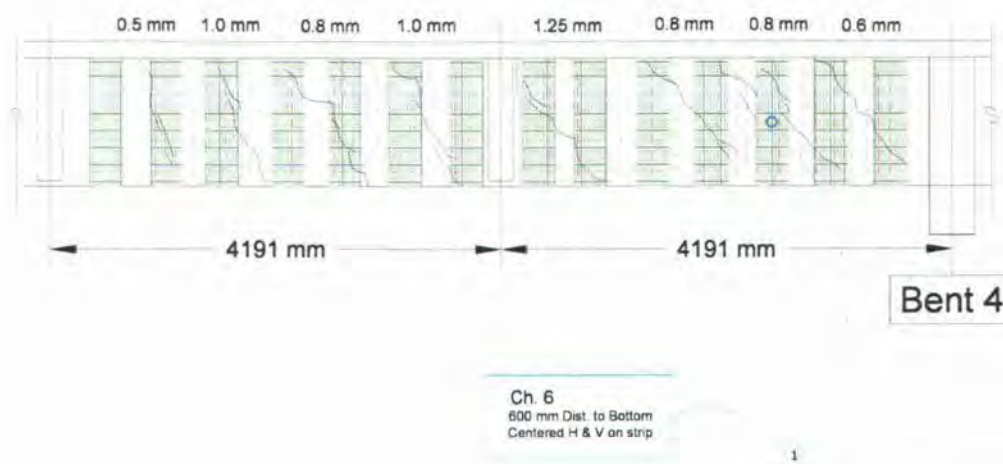


Fig. 3.3: Field measured cracking, embedded stirrups, and externally bonded CFRP on exterior girder

After inspection, strain gages were installed on individual CFRP strips at selected high-shear locations. Strain gages were bonded to the surface of the CFRP at mid-depth of the girder and oriented in the vertical (fiber) direction. The chosen strain gage had a gage length of 51 mm (2 in.), permitting strain averaging over several transverse weave fibers that were spaced approximately 8 mm (0.31 in.). Instrumented locations are illustrated schematically in Fig. 3.4. The strain gages were connected to a Campbell Scientific CR9000 data logger, a high-speed, multi-channel, 16-bit digital data acquisition system. To reduce noise and prevent aliasing in the data, both analog and digital filters were employed. During the ambient monitoring period, data were sampled at 100 Hz. A digital high-pass filter was utilized with a cut-off frequency of 40 Hz. The

system recorded sensor readings and converted signals into corresponding CFRP strains. Data from sensors were archived for retrieval and post-processing.

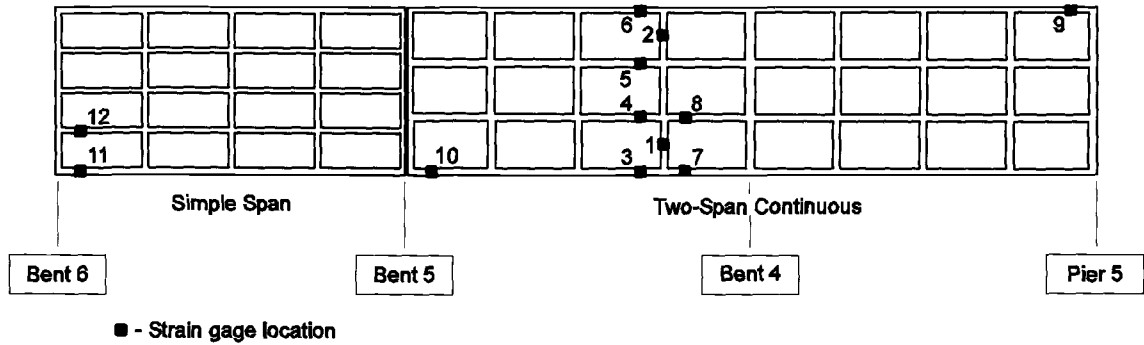


Fig. 3.4: Schematic of instrumentation locations

Ambient Traffic Induced CFRP Strains

Ambient traffic induced CFRP strains at mid-depth of the girders and bent cap were monitored over a period of 32.6 days. The strain ranges and numbers of cycles recorded at the instrumented locations are shown in Fig. 3.5. The largest single strain range was measured at approximately $34 \mu\epsilon$ for location #2 on the bent cap. Using Miner's Rule (Miner, 1945), the variable amplitude strains were described as an equivalent constant amplitude strain-range for each of the instrumented locations:

$$SR_{eqv} = \sqrt[3]{\sum \frac{n_i}{N_{tot}} SR_i^3} \quad (3.3)$$

where SR_i is the i^{th} strain-range, n_i is the number of cycles observed for the i^{th} strain range, and N_{tot} is the total number of cycles at all strain ranges. The equivalent constant amplitude strain ranges were below $9 \mu\epsilon$ at all locations as shown in Fig. 3.6.

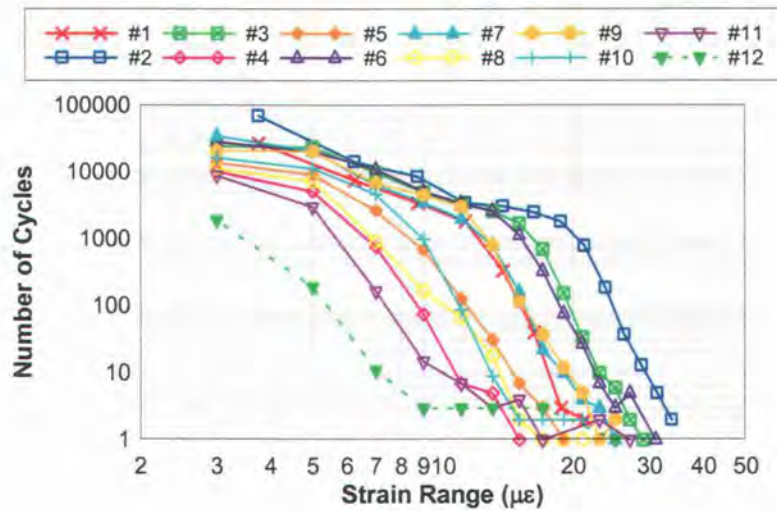


Fig. 3.5: Strain range-number of cycles measured under ambient traffic conditions at all instrumented locations

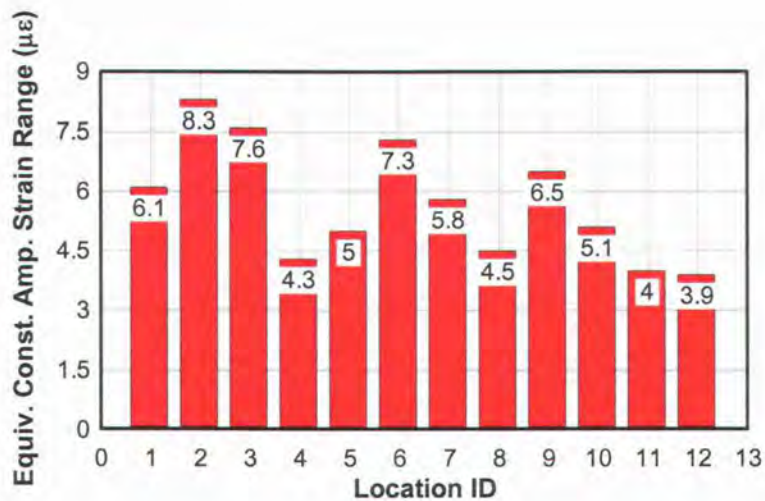


Fig. 3.6: Equivalent constant amplitude strain ranges for all instrumented locations

Field-measured strain ranges and numbers of cycles for each instrumented location were used to determine an equivalent strain range for laboratory fatigue specimens. To simulate the effects of high-cycle fatigue in laboratory specimens, 1,000,000 cycles of repeated loading was selected to produce equivalent damage in a reasonably short

period of time. The strain range required to produce equivalent damage in laboratory specimens at 1,000,000 cycles, as that measured in the field over a projected period of 10, 20, and 50 years, was estimated by computing an equivalent strain range per Eqn. 3 using the location exhibiting the highest strain ranges (location #2). It was assumed that the field measured CFRP strain ranges and numbers of cycles remain constant over the extended life of the bridge. The CFRP strain ranges required to approximate in-situ damage for the laboratory specimens were 19, 24, and 32 $\mu\epsilon$ for 10, 20, and 50 year service lives, respectively. Laboratory tests of full-size girder specimens with 1950's vintage proportions were initially loaded until cracked, repaired with CFRP, and subjected to high-cycle service-level loads approximating those observed in the field to produce equivalent damage. These laboratory tests and results are reported subsequently.

Laboratory Tests

Test Specimens

Five specimens were tested as part of the experimental investigation. Two control specimens were tested monotonically and three under fatigue loading. Specimens were designed to reflect 1950's vintage proportions, materials, and details at full scale based on previous work done by Higgins *et al.* (2004). Two designs were used to test both positive (T-beam) and negative moment bending regions (inverted-T (IT)) with various flexural bar cut-off, hook, and stirrup spacing details as seen in Fig. 3.7. Specimens were initially loaded to produce diagonal cracking representative of that observed in

field inspections of existing Oregon highway bridges. They were then repaired with CFRP, fatigued for 1 million cycles (except the control specimens), and then tested to failure.

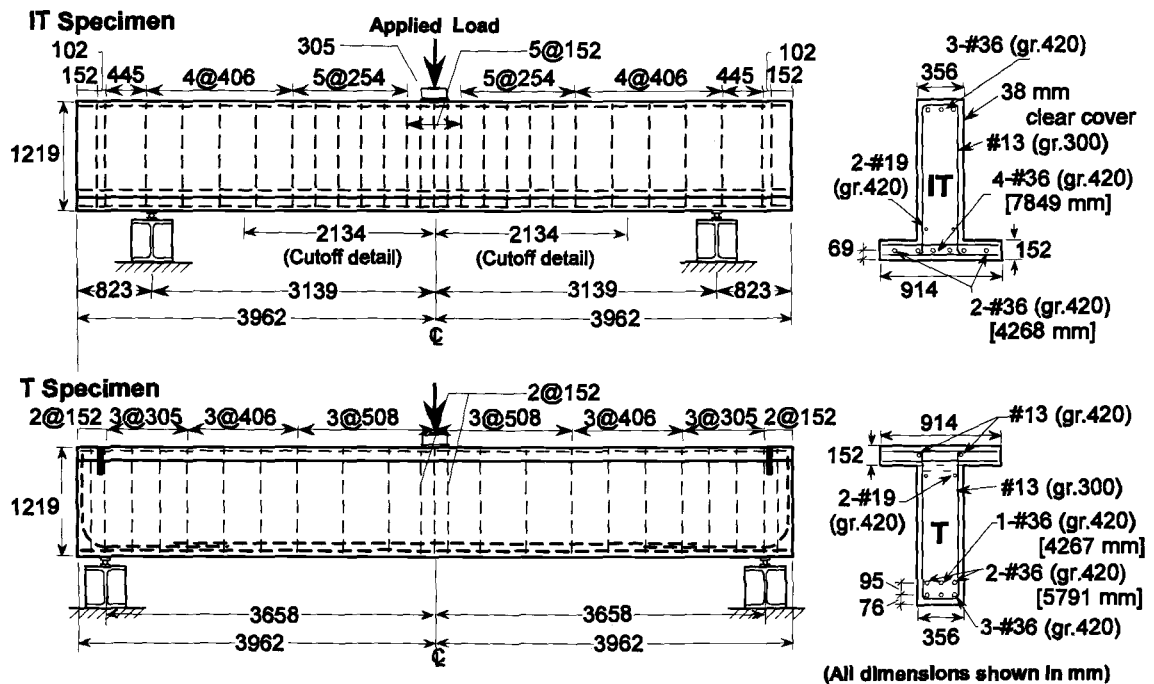


Fig. 3.7: Typical specimen details

All specimens were cast with the same cross-sectional geometry. Members had a height of 1219 mm (48 in) with a stem width of 356 mm (14 in) and a deck portion 914 mm (36 in) wide by 152 mm (6 in) thick as depicted in Fig. 3.7. Reinforcing bars for all of the specimens were from the same heats and tension tests were conducted to determine material properties as summarized in Table 3.1. ASTM A615 Grade 420 (60 ksi) steel was used for the longitudinal reinforcing, with Grade 300 (40 ksi) steel for the stirrups. The stirrup grade is representative of intermediate grade steel used in the 1950's. A

concrete mix design was used which produced compressive strengths similar to ODOT specified compressive strengths of around 24 MPa (3500 psi). The 28-day and day-of-test cylinder strengths are shown in Table 3.2.

Table 3.1: Steel reinforcing property description

Description	Bar Size	Grade	f_y (MPa)	f_{ult} (MPa)
Stirrups	# 13	300	350	559
Deck	# 13	420	443	724
Skin	# 19	420	461	648
Flexure	# 36	420	481	717
Hooks	# 36	420	481	717

Table 3.2: Concrete and CFRP bond properties and maximum initial diagonal crack size

Specimen	f'_c (MPa)		Initial Max Crack Size (mm)	CFRP Bond Strength (MPa)
	28-Day	Failure		
2T04	26.27	29.37	0.762	1.82
2T03	23.17	25.40	0.762	2.83
1IT02	26.27	26.34	1.016	2.02
3IT05	23.48	25.39	1.016	2.15
3IT06	22.70	23.33	0.762	1.81

All repairs were done using unidirectional high strength carbon fiber fabric applied in a wet lay-up procedure. Two different fibers were used with individual component and composite properties shown in Table 3.3. Composite properties were determined from unidirectional tension tests performed for each fiber thickness per ASTM 3039 recommendations. The same materials were used on the laboratory specimens as were

used in the repair of the field study bridge, and were both done by the same approved applicator.

Table 3.3: Composite material properties: Reported and experimental

Property	Individual Component*			Composite [†]			
	Saturant	Carbon Fiber		CF130		CF160	
		CF130	CF160	Mean	St Dev	Mean	St Dev
Thickness, t (mm/ply)	-	0.165	0.33	0.975	0.134	1.47	0.16
Ultimate Tensile Strength (MPa)	55.2	3800	3800	717	94	846	151
Ultimate Tensile Strength per Unit Width (kN/mm/ply)	-	0.625	1.25	0.692	0.042	1.22	0.13
Tensile Modulus (MPa)	3034	227000	227000	38750	4530	54400	7020
Ultimate Rupture Strain, %	3.5	1.67	1.67	1.85	0.11	1.55	0.18

*Master Builders, Inc. 2001 material vendor specifications.

[†]Average and standard deviation values obtained from 20 composite samples of each fiber type tested in accordance with ASTM D 3039/D 3039M.

Test Variables

All tests were conducted using a three-point loading configuration. Precrack and failure tests were done in a setup as shown in Fig. 3.8. Load was applied through a 3560 kN (800 kip) capacity hydraulic cylinder operating on a 69 MPa (10,000 psi) system. The applied force was measured with a 2670 kN (600 kip) capacity load cell. Fatigue loading was performed using load-control in a setup shown in Fig. 3.9. Force was applied through a 980 kN (220 kip) capacity hydraulic actuator operating on a 21 MPa (3000 psi) system. Applied force was measured with a 980 kN (220) kip load cell. Load was distributed through a 25 mm (1 in) thick 305 mm (12 in) square steel plate in both setups. End reactions were applied through 102 mm (4 in) wide steel plates resting on

51 mm (2 in) diameter steel rollers, fastened to steel spreader beams attached to the laboratory strong-floor. High-strength grout was applied to the contact surfaces between the steel plates and specimens to ensure level and even bearing areas. Inverted-T (IT) specimens were tested at a span length of 6280 mm (20.6 ft) between centerline of supports for both precrack and failure loading schemes and at 7315 mm (24 ft) span for fatigue. T-beams were tested at 7315 mm (24 ft) spans for all three loading phases.

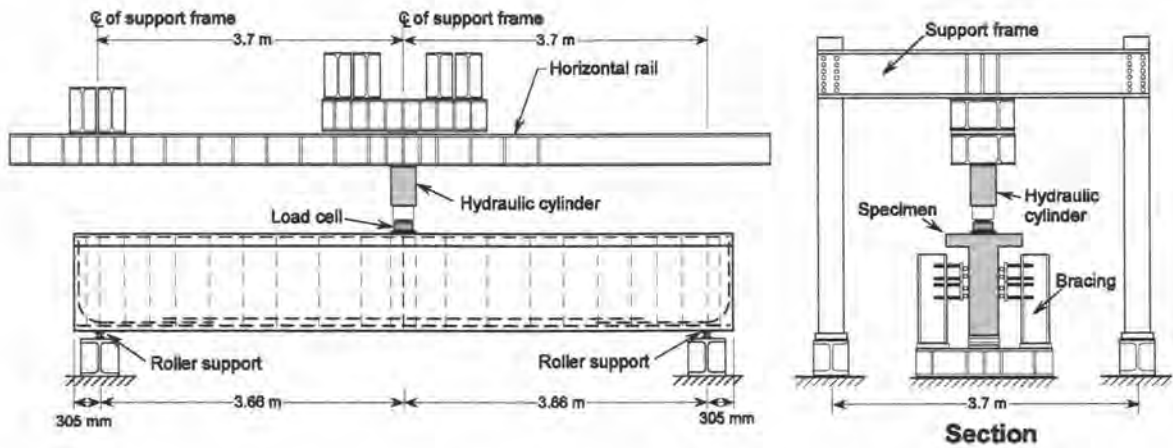


Fig. 3.8: Precrack and failure test setup

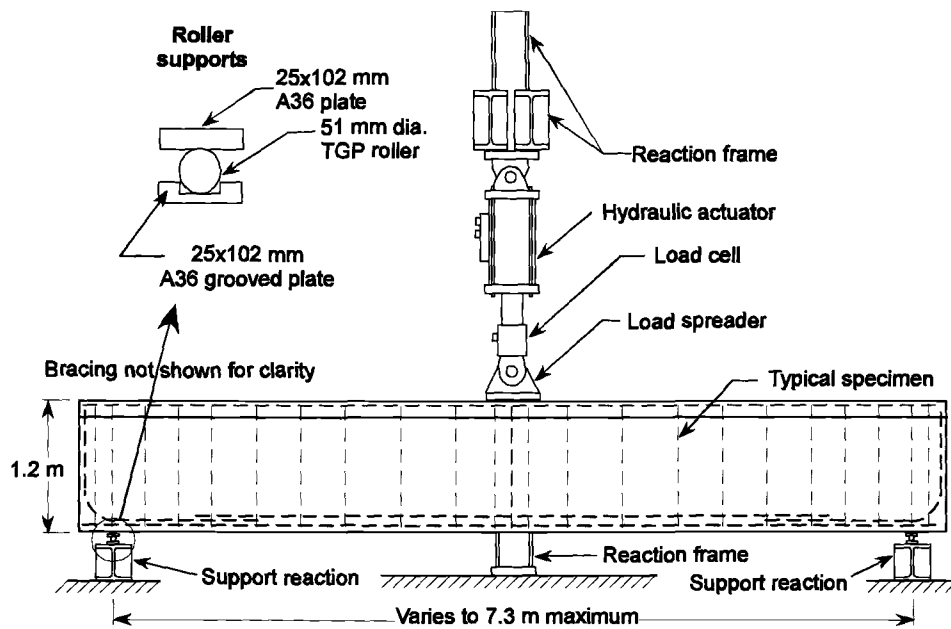


Fig. 3.9: Fatigue test setup

Instrumentation was applied to each specimen to capture local and global behaviors. Strain gages were used to monitor internal steel reinforcing and external CFRP strains, displacement transducers were used to measure diagonal deformations, local crack motions, and support displacements at each corner of the reaction plates, and string potentiometers to measure centerline displacement. Typical instrumentation is shown in Fig. 3.10.

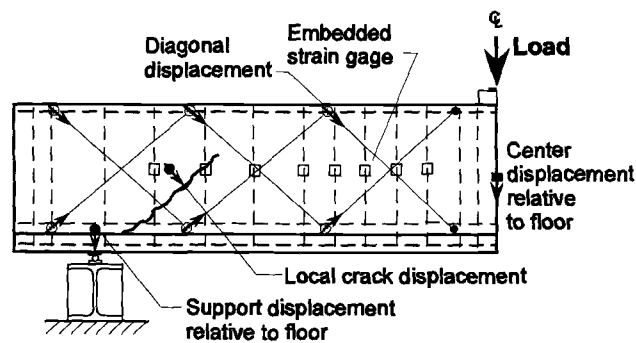


Fig. 3.10: Typical instrumentation layout

Testing Method

The initial loading protocol carried out on each specimen was performed to induce diagonal cracking representative of in-service CRC girders. Load was applied incrementally at 222 kN (50 kips) to a level of 1112 kN (250 kips) for T specimens and 1334 kN (300 kips) for IT specimens with removal of load between each step. Maximum crack sizes after loading of each beam are shown in Table 3.2, and ranged from 0.08 – 1.0 mm (0.03 – 0.04 in). After reaching the desired level of cracking, the applied load was removed.

Once girders were diagonally cracked, a commercially available CFRP unidirectional high strength carbon fiber fabric laminate system was applied to the specimens. The entire repair procedure was performed by a qualified contractor with experienced personnel. Cracks were inspected and all significant diagonal cracks were injected with a high strength epoxy resin and allowed to cure. Not all visible cracks were injected, just those of sufficient width to permit the epoxy to flow between the crack surfaces. The beams were then surfaced with a diamond bit grinder to remove loose concrete and expose voids. A primer was spread over areas to be applied with CFRP and once dry, a putty and saturant were applied. While both were wet, the carbon fiber was cut and applied to the specified locations, being worked into place with a soft trowel until the saturant made its way through the fibers. A final layer of saturant was then applied.

Upon reaching the manufacturers recommended curing times, the specimens were instrumented, fatigued (except 1IT02 and 2T04), and tested to failure. U-wrap laminate locations on each specimen are shown in Fig. 3.11. A 406 mm (16 in) space in the center of each IT specimen was included to simulate the bent cap location in a bridge structure where it is not possible to apply the CFRP. Specimens 1IT02, 3IT05, and 3IT06 were repaired with a single layer of 305 mm (12 in.) wide CF130 laminate spaced 256 mm (14 in.) on center. Specimens 2T03 and 2T04 were repaired with a single layer of 254 mm (10 in.) wide CF160 laminate spaced 256 mm (14 in.) on center.

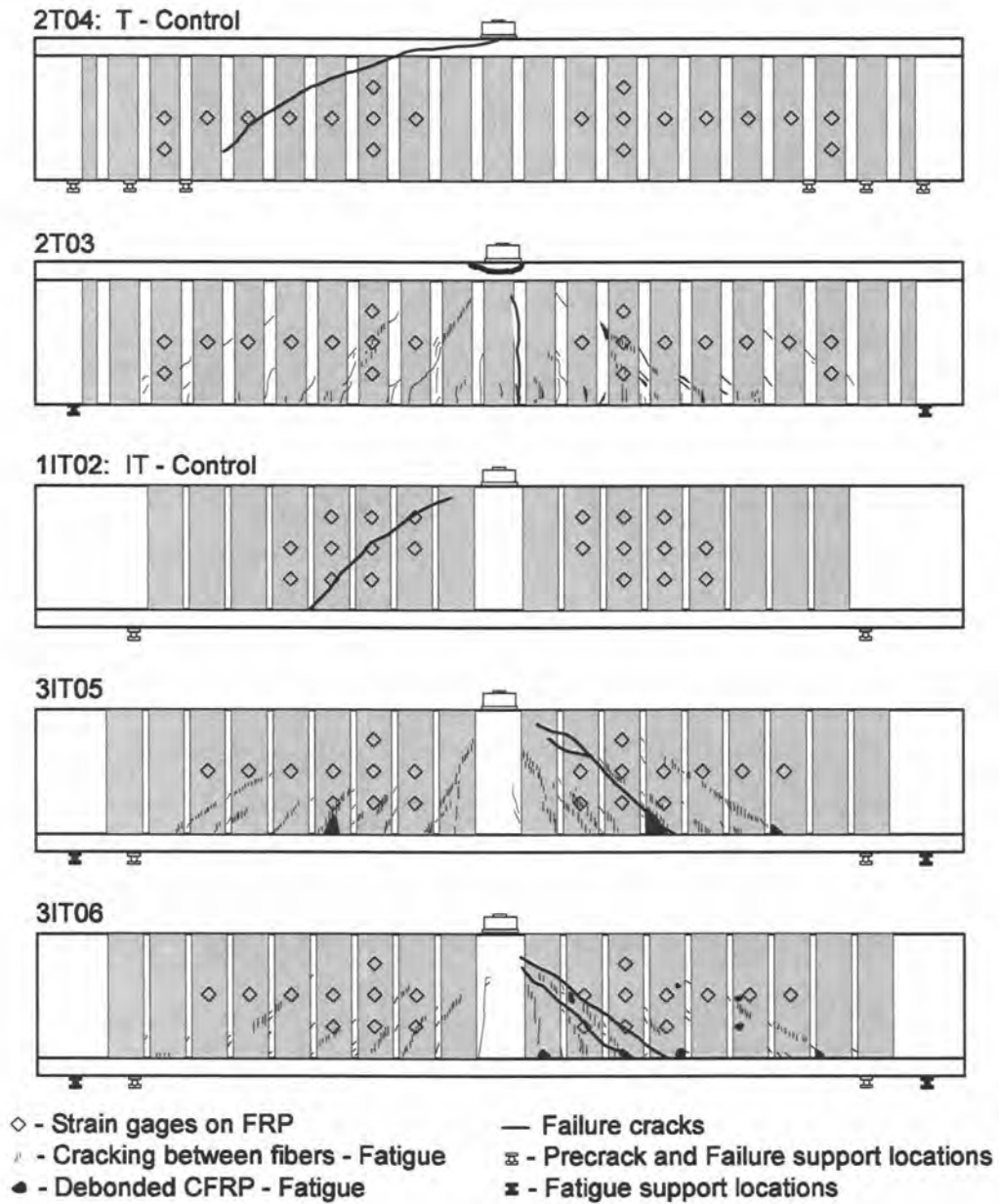


Fig. 3.11: CFRP repair layout, fatigue damage, and failure cracks and debonding

After repair, the specimens were subjected to an initial overload prior to beginning high-cycle fatigue loading. An incremental load program was conducted from zero to 890 kN (200 kips) at 222 kN (50 kips) steps with unloading. Reaching the peak overload condition resulted in diagonal cracking visible between individual u-wraps. This worst-case scenario of a significant initial load sufficient to cause cracking creates higher stresses in the embedded rebar (both flexural and stirrups) as well as in the CFRP and facilitates bond fatigue.

Fatigue loading was conducted using a sinusoidal loading function with unique load ranges for each specimen to obtain target damage for one million cycles. The T specimen 2T03 was fatigued at a load range of 445 kN (100 kips) with a mean of 267 kN (60 kips) at a frequency of 1.25 Hz. Specimen 3IT05 was fatigued at a load range of 800 kN (180 kips) at 1.0 Hz and 3IT06 at 489 kN (110 kips) and 1.25 Hz, with means of 445 kN (100 kips) and 334 kN (75 kips), respectively. Consideration was taken to limit measured strains of the internal steel reinforcing to ensure levels were below the fatigue limit of 165 MPa (24 ksi) at one million cycles. This was done to preclude rebar metal fatigue, and only incorporate effects of rebar bond fatigue and CFRP material and bond fatigue that can reasonably occur at service-level conditions based on field measured bridge response described previously and further detailed by Higgins *et al.* (2004).

All specimens were loaded in 222 kN (50 kip) increments from zero to failure with removal of load to 22 kN (5 kips) each cycle. Peak applied shear force at failure is

shown in Table 3.4 as V_{APP} for each specimen. Also shown, is the amount of member self weight contributing to the shear failure labeled as V_d because specimen sizes for these tests have a significant self-weight contribution. Self-weight was calculated based on the amount of concrete below the failure crack. The summation of the applied shear and the self-weight shear forces yields the total failure shear force, V_{EXP} .

Table 3.4: Experimental summary

Specimen	Fatigue Load Range (kN)	Failure Mode	V_{APP} (kN)	V_d (kN)	V_{EXP} (kN)	θ_{ck} (deg)
2T04	-	Shear / Compression	1228	18.3	1246	40
2T03	445	Flexure	956	-	956	90
1IT02	-	Shear / Compression	1112	12.7	1125	37
3IT05	800	Shear / Compression	1134	13.0	1147	45
3IT06	490	Shear / Tension	1116	9.3	1126	39

Experimental Results

The performance of the repairs was evaluated through load-deflection response, internal rebar and external CFRP strains, flexural reinforcement demand, and diagonal crack growth. Global and local demands were compared before and after the specimens were fatigued to determine changes over one million cycles of repeated load. Debonding of the CFRP u-wraps and crack propagation were also monitored during tests.

Ultimate strength capacity of fatigue specimens with comparable unfatigued specimens showed that the fatigue loading did not significantly affect capacity, as shown in Table 3.4. There were observed differences between specimens and changes were noted for local and global deformations and strains during fatigue testing.

IT specimens produced additional overall displacement under fatigue loading as progressive debonding of the CFRP strips and internal stirrups occurred. The T specimen did not exhibit changes in overall displacement as shown in Fig. 3.12. The higher load range produced softening in specimen 3IT05, comparing the start and end of fatigue testing. Changes in local diagonal crack widths were observed during fatigue as shown in Fig. 3.13. It was evident that the higher load range produced larger diagonal crack opening after one million cycles than the lower load range. Diagonal deformation response within a section of the shear span of the IT specimens also showed similar results. The deformation responses of a section 1067 mm (42 in) wide by 991 mm (39 in) high in the same location on the stem for the control and two fatigue IT specimens are shown in Fig. 3.14. The control specimen 1IT02 was much stiffer with negligible deformation up to 1000 kN (225 kips) of applied force. Specimens 3IT06 and 3IT05 experienced greater deformations, respectively, than the control at corresponding loads. This trend continued through most of the load-deformation response until the load began to approach ultimate. At ultimate, all of the diagonal deformation magnitudes were similar, and all failed at approximately the same applied shear force as shown in Table 3.4.

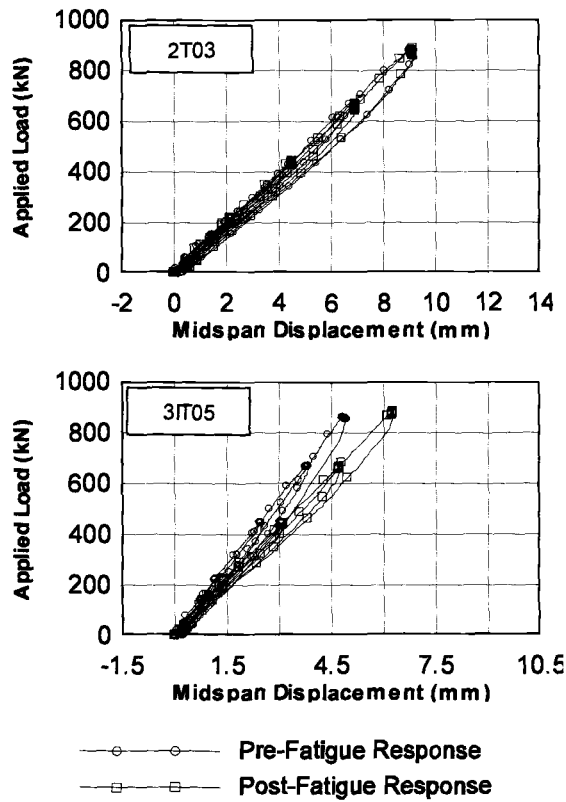


Fig. 3.12: Midspan displacement response comparison of specimens prior to and after fatigue loading

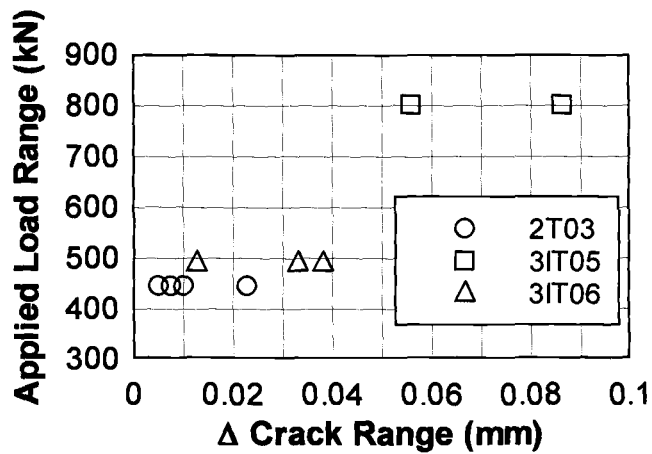


Fig. 3.13: Change in crack size range for various fatigue loading ranges

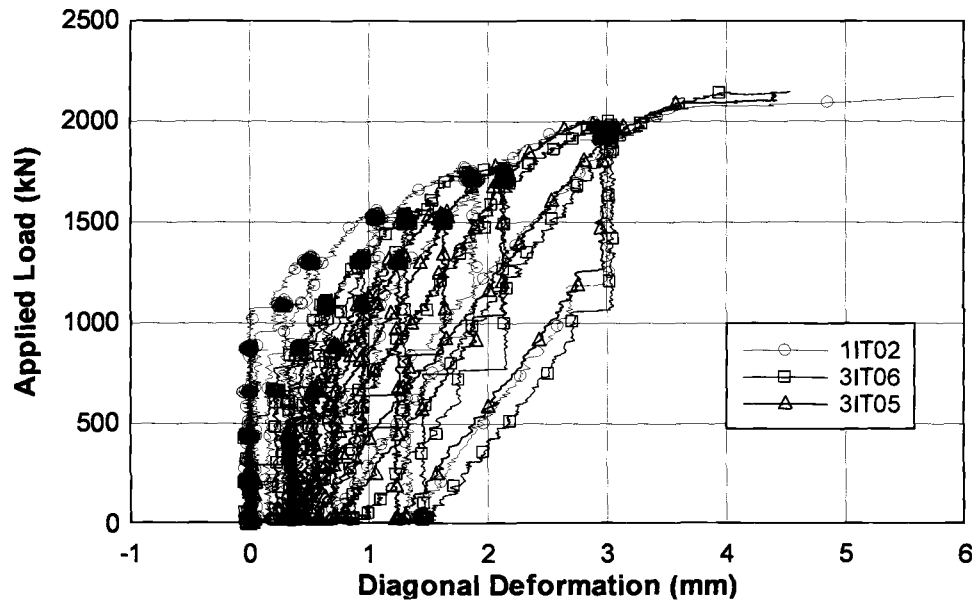


Fig. 3.14: Diagonal deformation response of IT specimens

In the fatigue specimens, diagonal cracks had already developed during the initial reload after repair and been worked during the fatigue loading. This allowed greater deformations to occur at corresponding loads due to local CFRP debonding and stirrup bond fatigue (between concrete and stirrup legs) associated with the diagonal crack locations. The IT fatigue specimens also contained regions of debonded CFRP material at the strip termination at the flexural tension region along the deck/stem interface. These locally debonded areas were sufficiently small so that as higher loads were reached during failure tests the member capacity was not impacted. Indeed, there was no marked change in the visual condition at the onset of failure between fatigued and unfatigued specimens. Failure was controlled for all specimens by bond failure as the CFRP u-wraps peeled away from the web, allowing diagonal cracks to propagate. The

exception was specimen 2T03, which failed in flexure without CFRP debonding. No fiber rupture was observed for any of the specimens.

The intent of a CFRP retrofit for shear is to extend the service life of the member by providing additional capacity and/or reducing demand on the internal reinforcing steel. Comparison of the stirrup and flexural rebar strains before application of CFRP and during failure testing after fatigue showed that the CFRP material tended to decrease the stirrup demands, particularly when the initial stirrup strain was large (those that would control the performance), as shown in Fig. 3.15. Application of the CFRP strips for shear did not significantly change the flexural steel demands at the cut-off locations.

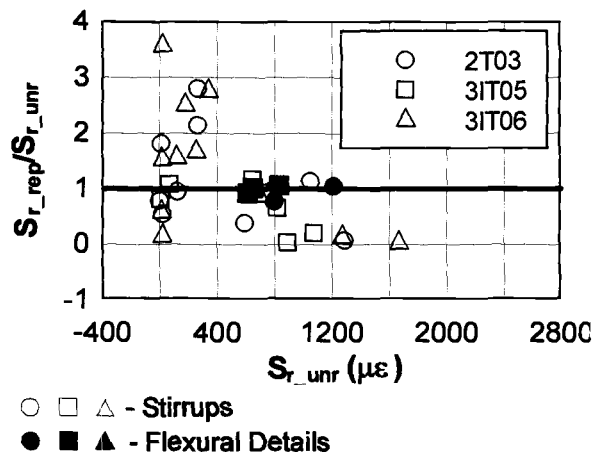


Fig. 3.15: Internal steel reinforcing strain reduction due to application of CFRP shear repair

Representative strain behavior of the stirrups at mid-height of an IT member and of CFRP u-wraps at mid-height and in the flexural tension zone are shown in Fig. 3.16.

The stirrup strain near mid-height is shown at a location near the eventual failure crack

region. The stirrup strain range was far below the threshold of $830 \mu\epsilon$ based on Eqn. 3.1 for inducing metal fatigue over one million cycles. In the T-beam specimen, shear demand was sufficiently low so that the stirrups showed very little change in strain throughout fatigue loading, and several showed a slight decreasing trend. The stirrup strain ranges were all well below the threshold required for long life.

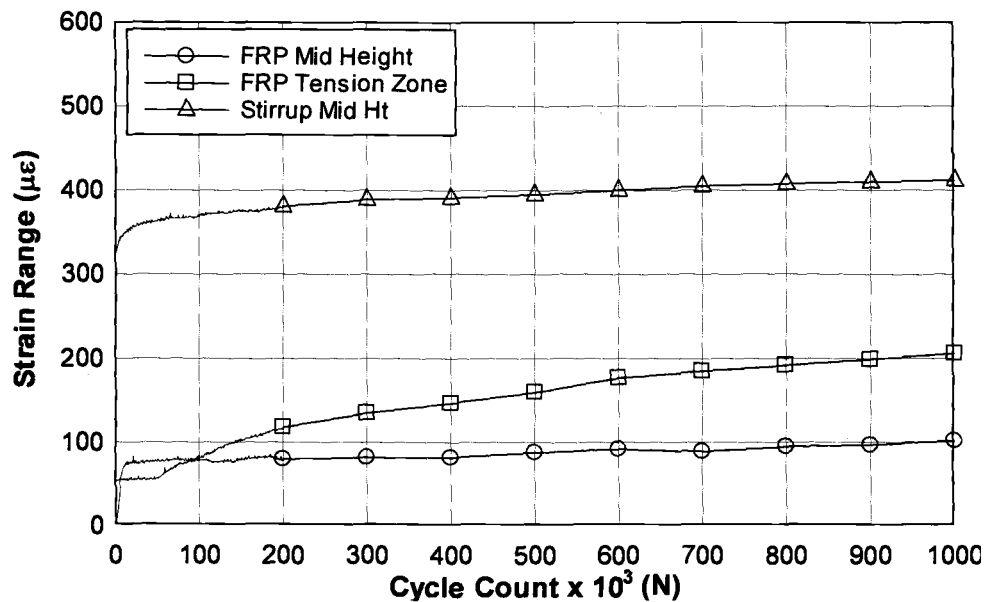


Fig. 3.16: Representative strains measured during fatigue loading

Strain response in the CFRP under fatigue varied depending on the instrument location relative to diagonal cracks and strip termination locations along the deck/stem interface. CFRP strain ranges near diagonal cracks tended to exhibit a nonlinear response, with strains increasing at a higher rate during initial fatigue cycles and then gradually increasing at a lower rate, as shown in Fig. 3.16. CFRP strains measured closer to the flexural tension zone near the terminated edge of the u-wraps trended upwards at a

higher rate in early cycles and gradually moved towards a steady-state. For the CFRP strain gage near the edge shown in Fig. 3.16, strain ranges during the initial cycles were unchanged because no cracks or CFRP debonding had yet propagated near the gage location. Once a crack propagated or debonding progressed (typically early in the fatigue history), the CFRP strain range increased at an initially high rate and then began to slow as stresses were redistributed, cracking does not continue to propagate, and debonding slows. The observed initial plateau does not necessarily exist, if the u-wrap bond to the surface of the specimen is near initial cracks or debonded prior to fatigue cycling. The representative strain at mid-height of the CFRP u-wraps exhibited a different behavior. The CFRP strain gage location shown was near a diagonal crack visible on both sides of the u-wrap. Strain range in the CFRP increased at the onset of fatigue cycling and then reached a near stationary value. During fatigue loading, diagonal cracks opened and closed. The crack surfaces wear against each other and small pieces of concrete at the crack interface may ravel and fall into the crack. This debris does not allow the crack to close and produced some small additional strain observed as an increase in the mean strain value. At the same time, the CFRP u-wraps gradually and locally debonded from the concrete surface while the stirrup legs undergo bond fatigue whereby the stirrup provides less constraint across the diagonal crack. Eventually near steady-state conditions were reached, and the strain ranges became almost constant. However, the observed strain ranges did not reach true steady-state conditions, and it may be projected that the CFRP debonding and stirrup bond fatigue continue to occur. Based on the level of CFRP debonding observed prior to failure in

the control specimens, very substantial debonding must occur before it significantly impacts ultimate capacity. It would be anticipated that this substantial and visually apparent debonding would be identified during routine and regular bridge inspections.

Progressive debonding of the CFRP strips produced a very fine concrete powder along the deck/stem interface in the flexural tension zone of the IT specimens. Accumulation of the gray powdery material was visible on the deck and developed more rapidly during early fatigue cycles and then slowly decreased. This was not the case with the T-beam specimen as the terminated edge of the u-wraps was not located in a flexural tension zone, and thus the demand at the strip termination edges was sufficiently low so that debonding did not occur. Identification of debonding of the CFRP u-wraps from the concrete surface was relatively easy using infrared thermography and also by sounding or tapping the CFRP surface. Compared with an adequately bonded area, the debonded areas tended to have a lower, hollow sound when tapped. Also observed during fatigue loading were vertical splitting cracks between the individual fibers of the CFRP u-wraps over diagonal cracks. These cracks were occasionally accompanied with local debonding, and often extended only a few centimeters vertically, as shown in Fig. 3.11. It should be noted that the observed fatigue-induced CFRP cracking and debonding did not significantly affect the capacity of the members as seen in Table 3.4.

Conclusions

Field tests were performed on an in-service RCDG bridge that had exhibited diagonal cracking and was retrofitted with CFRP shear reinforcing. The bridge was inspected and CFRP u-wraps were instrumented. Strain ranges in CFRP strips were measured under ambient traffic conditions and equivalent constant amplitude strain ranges were determined. The field data provided a baseline for laboratory tests to determine the impact of repeated loading on strength and behavior of RCDG bridge members repaired with CFRP for shear. Positive and negative bending moment regions were investigated and the effect of different fatigue load ranges were considered. Based on the field inspections and tests and subsequent laboratory investigation, the following conclusions are presented:

- Under ambient traffic loading, the single largest field measured strain range for an instrumented CFRP strip was approximately $34 \mu\epsilon$.
- Based on ambient traffic induced strain ranges, an equivalent strain range was determined for each of the instrumented locations. The equivalent constant amplitude strain range was below $9 \mu\epsilon$ for all locations.
- Based on the highest field measured strain location, a CFRP strain range required to produce the estimated equivalence of 50 years of service-life damage in 1,000,000 cycles for laboratory specimens was determined as approximately $32 \mu\epsilon$.

- Service-level fatigue loading histories, above those observed in the field, did not produce significant changes in ultimate capacity for the specimens.
- Vertical CFRP strips reduced service-level stirrup stresses but did not reduce flexural steel stresses.
- Under repeated loading, small areas of the CFRP strips debonded along diagonal cracks and at the terminating edges of the strips at the deck/stem interface. Field inspections for debonded regions should focus on these regions.
- A gap between adjacent CFRP strips permitted identification of diagonal cracking in the girder after repair and is recommended for future installations to facilitate biennial bridge inspections.
- Debonded areas of CFRP material were easily identified by infrared thermography or by sounding the CFRP material and listening for a change in sound frequency.
- Failure was controlled by debonding of CFRP strips initiating near the deck/stem interface for both fatigued and unfatigued IT specimens. No substantial visual differences between fatigued and unfatigued specimens prior to failure were observed.
- Terminating edges of the CFRP strips located near the compression zone did not exhibit debonding under fatigue load.

- Diagonal crack motions increased under repeated fatigue loading and the higher fatigue load range produced larger crack motions, although the capacity was not significantly affected.

Acknowledgements

This research was funded by the Oregon Department of Transportation and Federal Highway Administration and overseen by research coordinator Mr. Steven Soltesz. All repair materials and procedures were donated by MBrace of Cleveland, Ohio and Pioneer Waterproofing of Portland, Oregon with the help of Mr. Neil Antonini. The help of both of these individuals is greatly appreciated. Reinforcing steel and fabrication were donated by Cascade Steel Rolling Mills of McMinnville, Oregon and Farwest Steel of Eugene, Oregon, respectively. The authors would also like to thank Dr. Tanarat Potisuk, Mr. Richard Forrest, Mr. Thomas Schumacher, Ms. Michelle Chavez, and Ms. Angela Rogge for their assistance in experimental testing and data reduction. The findings and conclusions are those of the authors and do not necessarily reflect those of the project sponsors or the individuals acknowledged.

Notation

The following symbols are used in this paper:

f_{bond}	=	bond strength demand of CFRP on concrete surface (MPa);
f'_c	=	compressive strength of concrete (MPa);
f_{ult}	=	ultimate stress of internal reinforcing steel (MPa);
f_y	=	yield stress of internal reinforcing steel (MPa);
h	=	height of reinforcing deformation lug (mm);
r	=	radius of reinforcing deformation lug (mm);
n_i	=	number of cycles observed for the i^{th} strain range;
N_{tot}	=	total number of cycles at all strain ranges;
Sr_i	=	the i^{th} strain-range ($\mu\epsilon$);
Sr_{rup}	=	strain range of internal stirrup after CFRP repair ($\mu\epsilon$);
Sr_{unr}	=	strain range of internal stirrup before CFRP repair ($\mu\epsilon$);
SR_{eqv}	=	equivalent constant amplitude strain-range ($\mu\epsilon$);
St Dev	=	standard deviation of measured CFRP properties;
V_{APP}	=	applied shear from actuator (kN);
V_{Pred}	=	predicted shear capacity using <i>Response 2000™</i> (kN);
Δ	=	change in magnitude (mm);
$\mu\epsilon_{\text{max}}$	=	maximum measured CFRP strain at mid height of u-wrap ($\mu\epsilon$);
θ_{ck}	=	angle of diagonal failure crack (degrees);
σ_{min}	=	minimum stress in reinforcing bar (MPa); and
σ_r	=	service level stress range (MPa).

References

AASHTO (American Association of State Highway Officials), (1941, 1944, 1949, 1953, 1957, 1961, 1965). "Standard Specifications for Highway Bridges." 3rd to 9th Editions, AASHTO, Washington, D.C.

AASHTO, (2002) "Standard Specification for Highway Bridges." 17th Edition." AASHTO, Washington, D. C.

ACI 318-63, (1963). "Building Code Requirements for Structural Concrete." American Concrete Institute, Detroit, Michigan.

ACI 318-02, (2002). "Building Code Requirements for Structural Concrete." American Concrete Institute, Farmington Hills, Michigan.

ACI Committee 215R-92 (1992). "Considerations for Design of Concrete Structures Subjected to Fatigue Loading." American Concrete Institute, Detroit, Michigan.

ACI SP-41 (1974). *Abeles Symposium - Fatigue of Concrete*. American Concrete Institute, Detroit, Michigan.

ACI SP-75 (1982). *Fatigue of Concrete Structures*. S.P. Shah (editor), American Concrete Institute, Detroit, Michigan.

ACI 440.2R-02, (2002). "Guide for the Design and Construction of Externally Bonded FRP Systems for Strengthening Concrete Structures." American Concrete Institute, Farmington Hills, Michigan.

ASTM A305-50T, (1950). "Tentative Specifications for Minimum Requirements for the Deformations of Deformed Steel Bars Concrete Reinforcement." ASTM, Philadelphia, PA.

ASTM D 3039/D 3039M-00, (2001). "Standard Test Method for Tensile Properties of Polymer Matrix Composite Materials." ASTM, West Conshohocken, PA.

Balazs, G.L., (1998). "Bond Under Repeated Loading." SP 180-6: Bond under Repeated Loading, A Tribute to Dr. Peter Gergely, Leon, R. (Editor), American Concrete Institute, Farmington Hills, Michigan, pp. 125-143.

Breña, S.F., Benouaich, M.A., Kreger, M.E., and Wood, S.L., (2005). "Fatigue Tests of Reinforced Concrete Beams Strengthened Using Carbon Fiber-Reinforced Polymer Composites." *ACI Structural Journal*, v. 102, No. 2, March-April, pp. 305-313.

Chang, T.S. and C.E. Kesler, (1958). "Static and Fatigue Strength in Shear of Beams with Tensile Reinforcement." *Journal of the American Concrete Institute*, Vol. 29, No. 12, pp. 1033-1053.

Corley, W.G., Hanson, J.M., and T. Helgason, (1978). "Design of Reinforced Concrete for Fatigue." *Journal of the Structural Division, ASCE*, Vol. 104, No. ST6, pp. 921-932.

Hanson, J.M., Burton, K.T., and E. Hognestad, (1968). "Fatigue Tests of Reinforcing Bars – Effect of Deformation Pattern." *Journal of the PCA Research and Development Laboratories*, Vol. 10, No. 3, pp.2-13.

Hanson, J.M. and Hulsbos, C.L. and D.A. VanHorn, (1970). "Fatigue Tests of Prestressed Concrete I-Beams." *Journal of the Structural Division, ASCE*, Vol. 96, No. ST11, pp. 2443-2464.

Hanson, J.M., Somes, M.F. and T. Helgason, (1974). "Investigation of Design Factors Affecting Fatigue Strength of Reinforcing Steel – Test Program." *SP-41: Abeles Symposium - Fatigue of Concrete*, American Concrete Institute, Detroit, Michigan, pp. 71-106.

Hawkins, N.M. (1974). "Fatigue Characteristics in Bond and Shear of Reinforced Concrete Beams." *SP-41: Abeles Symposium - Fatigue of Concrete*, American Concrete Institute, Detroit, Michigan, pp. 203-236.

Helgason, T. and J.M. Hanson, (1974). "Investigation of Design Factors Affecting Fatigue Strength of Reinforcing Steel – Statistical Analysis." *SP-41: Abeles Symposium - Fatigue of Concrete*, American Concrete Institute, Detroit, Michigan, pp. 107-138.

Higgins, C., Miller, T.H., Rosowsky, D.V., Yim, S.C., Potisuk, T., Daniels, T.K., Nicholas, B.S., Robelo, M.J., Lee, A-Y, and R.W. Forrest, (2004). "Assessment Methodology for Diagonally Cracked Reinforced Concrete Deck Girders." *Report No. FHWA-OR-RD-05-04*, Federal Highway Administration, Washington, D. C.

Jhamb I.C. and J.G. MacGregor, (1974). "Effects of Surface Characteristics on Fatigue Strength of Reinforcing Steel." *SP-41: Abeles Symposium - Fatigue of Concrete*, American Concrete Institute, Detroit, Michigan, pp. 139-168.

Kreger, M.E., Bachman, P.M., and J.E. Breen, (1989). "An Exploratory Study of Shear Fatigue Behavior of Prestressed Concrete Girders." *PCI Journal*, July/August pp. 104-125.

Kwak, K-H. and J-G. Park, (2001). "Shear-Fatigue Behavior of High-Strength Concrete Under Repeated Loading." *Structural Engineering and Mechanics*, Vol. 11, No. 3, pp. 301-314.

Kwak, K-H., Suh, J., and C-Z., T. Hsu, (1991). "Shear-Fatigue Behavior of Steel Fiber Reinforced Concrete Beams." *ACI Structural Journal*, Vol. 88, No. 2, pp. 155-160.

Lopez, M.M., Naaman, A.E., Pinkerton, L., Till, R.D., (2003). "Behavior of RC Beams Strengthened with FRP Laminates and Tested Under Cyclic Loading at Low Temperatures." *International Journal of Materials and Product Technology*, v. 19, Nos. 1-2, pp. 108-117.

Master Builders, Inc., (2001). "MBrace Composite Strengthening System Material Specifications." Cleveland, OH.

Miner, M. A., (1945) "Cumulative Damage in Fatigue." *Journal of Applied Mechanics*, Vol. 12, Trans. ASME Vol. 67, pp. A159-A164.

Muszynski, L.C. and Sierakowski, R.L., (1996). "Fatigue Strength of Externally Reinforced Concrete Beams." *Proceedings of the Materials Engineering Conference*, v. 1, pp. 648-656.

Papakonstantinou, C.G., Petrou, M.F., Harries, K.A., (2001). "Fatigue Behavior of RC Beams Strengthened with GFRP Sheets." *Journal of Composites for Construction*, v. 5, No. 4, November, pp. 246-253.

Price, K.M. and A.D. Edwards, (1971). "Fatigue Strength in Shear of Prestressed Concrete I-Beams." *ACI Journal*, ACI, Vol. 68, April, pp. 282-292.

Rehm, G. and R. Eligehausen, (1979). "Bond of Ribbed Bars Under High-Cycle Repeated Loads." *ACI Journal*, Vol. 76, Feb., pp. 297-309.

Siess, C.P. (1960). "Research, Building Codes, and Engineering Practice." *ACI Journal*, May, ACI, pp. 1105-1122.

Tedesco, J.W., Stallings, J.M., El-Mihilmy, M., McCauley, M.W., (1996). "Rehabilitation of a Concrete Bridge Using FRP Laminates." *Proceedings of the Materials Engineering Conference*, v. 1, pp. 631-637.

Teng, S., Ma, W., Tan, K.H., and F.K. Kong, (1998). "Fatigue Tests of Reinforced Concrete Deep Beams." *The Structural Engineer*, Vol. 76, No. 18, pp. 347-352.

Ueda, T. and H. Okamura, (1983). "Behavior in Shear of Reinforced Concrete Beams under Fatigue Loading." *Journal of the Faculty of Engineering*, The University of Tokyo, Vol. 37, No. 1, pp. 17-48.

Ueda, T. and H. Okamura, (1981). "Behavior of Stirrup Under Fatigue Loading." *Transactions of the Japan Concrete Institute*, JCI, Vol. 3, pp. 305-318.

General Conclusion

Investigation of the performance of shear deficient CRC deck girders repaired with CFRP included laboratory tests conducted on eight specimens and field tests of an in-service 1950's vintage bridge. Data collected from field tests were used as a basis for design of repair schemes and loading protocol of fatigue specimens. Subsequent laboratory testing of specimens built to reflect 1950's vintage proportions, materials, and details was performed. Five specimens were tested at near static conditions and three specimens were fatigued prior to failure. Based on general experimental observations of performance, the following conclusions are presented:

- Specimen response after repair was noticeably stiffer in terms of midspan displacement and diagonal deformations.
- The repaired members exhibited strain compatibility between external CFRP strips and internal stirrups. Addition of the CFRP strips reduced the live-load demand in the internal stirrups at similar load levels.
- Repair for shear using CFRP must recognize the impact of the increased shear capacity on the flexural demands to prevent anchorage failures at flexural bar cut-off and anchorage details.
- Failure was controlled by debonding of CFRP strips initiating near the deck/stem interface.

- The CFRP repaired members tended to exhibit steeper crack angles than similar unrepaired specimens. At the point of failure, only one u-wrap was still acting across the failure crack.
- Prior to failure, significant areas of debonded CFRP material were observed. Progressive debonding of the multiple strips over the loading history provided a visual indication of distress prior to failure.
- Service-level fatigue loading histories, above those observed in the field, did not produce significant changes in ultimate capacity for the specimens.
- Under repeated loading, small areas of the CFRP strips debonded along diagonal cracks and at the terminating edges of the strips at the deck/stem interface. Field inspections for debonded regions should focus on these regions.
- A gap between adjacent CFRP strips permitted identification of diagonal cracking in the girder after repair and is recommended for future installations to facilitate biennial bridge inspections.
- Debonded areas of CFRP material were easily identified by infrared thermography or by sounding the CFRP material and listening for a change in sound frequency.

Bibliography

AASHO (American Association of State Highway Officials), (1941, 1944, 1949, 1953, 1957, 1961, 1965). "Standard Specifications for Highway Bridges." 3rd to 9th Editions, AASHO, Washington, D.C.

AASHTO, (2002) "Standard Specification for Highway Bridges." 17th Edition." AASHTO, Washington, D. C.

ACI 318-63, (1963). "Building Code Requirements for Structural Concrete." American Concrete Institute, Detroit, Michigan.

ACI 318-02, (2002). "Building Code Requirements for Structural Concrete." American Concrete Institute, Farmington Hills, Michigan.

ACI Committee 215R-92 (1992). "Considerations for Design of Concrete Structures Subjected to Fatigue Loading." American Concrete Institute, Detroit, Michigan.

ACI SP-41 (1974). *Abeles Symposium - Fatigue of Concrete*. American Concrete Institute, Detroit, Michigan.

ACI SP-75 (1982). *Fatigue of Concrete Structures*. S.P. Shah (editor), American Concrete Institute, Detroit, Michigan.

ACI 440.2R-02, (2002). "Guide for the Design and Construction of Externally Bonded FRP Systems for Strengthening Concrete Structures." American Concrete Institute, Farmington Hills, Michigan.

ASTM A305-50T, (1950). "Tentative Specifications for Minimum Requirements for the Deformations of Deformed Steel Bars Concrete Reinforcement." ASTM, Philadelphia, PA.

ASTM D 3039/D 3039M-00, (2001). "Standard Test Method for Tensile Properties of Polymer Matrix Composite Materials." ASTM, West Conshohocken, PA.

Al-Mahaidi, R., Lee, K., Taplin, G., (2001). "Behavior and Analysis of RC T-Beams Partially Damaged in Shear and Repaired with CFRP Laminates," Structures Congress, ASCE, Washington DC, May.

Balazs, G.L., (1998). "Bond Under Repeated Loading." SP 180-6: Bond under Repeated Loading, A Tribute to Dr. Peter Gergely, Leon, R. (Editor), American Concrete Institute, Farmington Hills, Michigan, pp. 125-143.

Bentz, E., (2000), Response 2000, University of Toronto,
<<http://www.ecf.utoronto.ca/~bentz/r2k.htm>>.

Breña, S.F., Benouaich, M.A., Kreger, M.E., and Wood, S.L., (2005). "Fatigue Tests of Reinforced Concrete Beams Strengthened Using Carbon Fiber-Reinforced Polymer Composites." *ACI Structural Journal*, v. 102, No. 2, March-April, pp. 305-313.

Chajes, M. J., Januszka, T.F., Mertz, D.R., Thomson, T.A., Finch, W.W., (1995). "Shear Strengthening of Reinforced Concrete Beams Using Externally Applied Composite Fabrics," *ACI Structural Journal*, v. 92, No. 3, May-June, pp. 295-303.

Chang, T.S. and C.E. Kesler, (1958). "Static and Fatigue Strength in Shear of Beams with Tensile Reinforcement." *Journal of the American Concrete Institute*, Vol. 29, No. 12, pp. 1033-1053.

Chen, J.F., Teng, J.G., (2003). "Shear Capacity of Fiber-Reinforced Polymer-Strengthened Reinforced Concrete Beams: Fiber Reinforced Polymer Rupture," *ASCE Journal of Structural Engineering*, v. 129, No. 5, May, pp. 615-625.

Corley, W.G., Hanson, J.M., and T. Helgason, (1978). "Design of Reinforced Concrete for Fatigue." *Journal of the Structural Division*, ASCE, Vol. 104, No. ST6, pp. 921-932.

Czaderski, C., EMPA, Swiss Federal Laboratories for Materials Testing and Research, (2000). "Shear Strengthening of Reinforced Concrete with CFRP," 45th International SAMPE Symposium, May 21-25, pp. 880-894.

Hanson, J.M., Burton, K.T., and E. Hognestad, (1968). "Fatigue Tests of Reinforcing Bars – Effect of Deformation Pattern." *Journal of the PCA Research and Development Laboratories*, Vol. 10, No. 3, pp.2-13.

Hanson, J.M. and Hulsbos, C.L. and D.A. VanHorn, (1970). "Fatigue Tests of Prestressed Concrete I-Beams." *Journal of the Structural Division*, ASCE, Vol. 96, No. ST11, pp. 2443-2464.

Hanson, J.M., Somes, M.F. and T. Helgason, (1974). "Investigation of Design Factors Affecting Fatigue Strength of Reinforcing Steel – Test Program." *SP-41: Abeles Symposium - Fatigue of Concrete*, American Concrete Institute, Detroit, Michigan, pp. 71-106.

- Hawkins, N.M., (1974). "Fatigue Characteristics in Bond and Shear of Reinforced Concrete Beams." *SP-41: Abeles Symposium - Fatigue of Concrete*, American Concrete Institute, Detroit, Michigan, pp. 203-236.
- Helgason, T. and J.M. Hanson, (1974). "Investigation of Design Factors Affecting Fatigue Strength of Reinforcing Steel – Statistical Analysis." *SP-41: Abeles Symposium - Fatigue of Concrete*, American Concrete Institute, Detroit, Michigan, pp. 107-138.
- Higgins, C., Miller, T.H., Rosowsky, D.V., Yim, S.C., Potisuk, T., Daniels, T.K., Nicholas, B.S., Robelo, M.J., Lee, A-Y, and R.W. Forrest, (2004). "Assessment Methodology for Diagonally Cracked Reinforced Concrete Deck Girders." *Report No. FHWA-OR-RD-05-04*, Federal Highway Administration, Washington, D. C.
- Jhamb I.C. and J.G. MacGregor, (1974). "Effects of Surface Characteristics on Fatigue Strength of Reinforcing Steel." *SP-41: Abeles Symposium - Fatigue of Concrete*, American Concrete Institute, Detroit, Michigan, pp. 139-168.
- Kachlakev, D., McCurry, D.D., (2000). "Behavior of Full-Scale Reinforced Concrete Beams Retrofitted for Shear and Flexural with FRP Laminates," *Composites Part B: Engineering*, v. 31, no. 6-7, pp. 445-452
- Kreger, M.E., Bachman, P.M., and J.E. Breen, (1989). "An Exploratory Study of Shear Fatigue Behavior of Prestressed Concrete Girders." *PCI Journal*, July/August pp. 104-125.
- Kwak, K-H. and J-G. Park, (2001). "Shear-Fatigue Behavior of High-Strength Concrete Under Repeated Loading." *Structural Engineering and Mechanics*, Vol. 11, No. 3, pp. 301-314.
- Kwak, K-H., Suh, J., and C-Z., T. Hsu, (1991). "Shear-Fatigue Behavior of Steel Fiber Reinforced Concrete Beams." *ACI Structural Journal*, Vol. 88, No. 2, pp. 155-160.
- Li, A., Assih, J., Delmas, Y., (2001). "Shear Strengthening of RC Beams with Externally Bonded CFRP Sheets," *ASCE Journal of Structural Engineering*, v. 127, No. 4, April pp. 374-380.
- Lopez, M.M., Naaman, A.E., Pinkerton, L., Till, R.D., (2003). "Behavior of RC Beams Strengthened with FRP Laminates and Tested Under Cyclic Loading at Low Temperatures." *International Journal of Materials and Product Technology*, v. 19, Nos. 1-2, pp. 108-117.
- Malvar, L.J., Warren, G.E., Inaba, C., (1995). "Rehabilitation of Navy Pier Beams with Composite Sheets," *Proceedings of the Second International RILEM Symposium*, August 23-25, pp. 533-540.

Master Builders, Inc., (2001). "MBrace Composite Strengthening System Material Specifications." Cleveland, OH.

Miner, M. A., (1945) "Cumulative Damage in Fatigue." *Journal of Applied Mechanics*, Vol. 12, Trans. ASME Vol. 67, pp. A159-A164.

Muszynski, L.C. and Sierakowski, R.L., (1996). "Fatigue Strength of Externally Reinforced Concrete Beams." *Proceedings of the Materials Engineering Conference*, v. 1, pp. 648-656.

Norris, T., Saadatmanesh, H., Ehsani, M.R., (1997). "Shear and Flexural Strengthening of R/C Beams with Carbon Fiber Sheets," *ASCE Journal of Structural Engineering*, v. 123, No. 7, July, pp. 903-911.

ODOT, "Oregon's Bridges 2002." Oregon Department of Transportation, <http://www.odot.state.or.us/tsbridgepub/PDFs/Senate_05_16_02.pdf> (May 16, 2002), Salem, Oregon.

Papakonstantinou, C.G., Petrou, M.F., Harries, K.A., (2001). "Fatigue Behavior of RC Beams Strengthened with GFRP Sheets." *Journal of Composites for Construction*, v. 5, No. 4, November, pp. 246-253.

Price, K.M. and A.D. Edwards, (1971). "Fatigue Strength in Shear of Prestressed Concrete I-Beams." *ACI Journal*, ACI, Vol. 68, April, pp. 282-292.

Rehm, G. and R. Eligehausen, (1979). "Bond of Ribbed Bars Under High-Cycle Repeated Loads." *ACI Journal*, Vol. 76, Feb., pp. 297-309.

Sato, Y., Ueda, T., Kakuta, Y., Tanaka, T., (1996). "Shear Reinforcing Effect of Carbon Fiber Sheet Attached to Side of Reinforced Concrete Beams," *Advanced Composite Materials in Bridges and Structures*, pp. 621-627.

Shehata, E., Morphy, R., Rizkalla, S., (2004). "Fibre Reinforced Polymer Shear Reinforcement for Concrete Members: Behaviour and Design Guidelines," *Canadian Journal of Civil Engineering*, v. 27, no. 5, October.

Siess, C.P., (1960). "Research, Building Codes, and Engineering Practice." *ACI Journal*, May, ACI, pp. 1105-1122.

Tedesco, J.W., Stallings, J.M., El-Mihilmy, M., McCauley, M.W., (1996). "Rehabilitation of a Concrete Bridge Using FRP Laminates." *Proceedings of the Materials Engineering Conference*, v. 1, pp. 631-637.

Teng, S., Ma, W., Tan, K.H., and F.K. Kong, (1998). "Fatigue Tests of Reinforced Concrete Deep Beams." *The Structural Engineer*, Vol. 76, No. 18, pp. 347-352.

Triantafillou, T.C., (1998). "Shear Strengthening of Reinforced Concrete Beams Using Epoxy-Bonded FRP Composites," *ACI Structural Journal*, v. 95, No.2, March-April, pp. 107-115.

Ueda, T. and H. Okamura, (1983). "Behavior in Shear of Reinforced Concrete Beams under Fatigue Loading." *Journal of the Faculty of Engineering*, The University of Tokyo, Vol. 37, No. 1, pp. 17-48.

Ueda, T. and H. Okamura, (1981). "Behavior of Stirrup Under Fatigue Loading." *Transactions of the Japan Concrete Institute*, JCI, Vol. 3, pp. 305-318.